



Technical Memorandum 80286

## Assessment of Shuttle Payloads Gaseous Environment

### Contamination and its Control with Application to the Cryogenic Limb-Scanning Interferometer Radiometer (CLIR)

(NASA-TM-80286) ASSESSMENT OF SHUTTLE  
PAYLOADS. GASEOUS ENVIRONMENT:  
CONTAMINATION AND ITS CONTROL WITH  
APPLICATION TO THE CRYOGENIC LIMB-SCANNING  
INTERFEROMETER RADIOMETER (CLIR) (NASA)

M84-70183

00/15 Unclass  
44335

**J. J. Scialdone**

**MAY 1979**

National Aeronautics and  
Space Administration

**Goddard Space Flight Center**  
Greenbelt, Maryland 20771

REPRODUCED BY  
NATIONAL TECHNICAL  
INFORMATION SERVICE  
U.S. DEPARTMENT OF COMMERCE  
SPRINGFIELD, VA. 22161



## BIBLIOGRAPHIC DATA SHEET

1. Report No. TM-80286	2. Government Accession No.	3. Recipient's Catalog No.	
4. Title and Subtitle Assessment of Shuttle Payloads Gaseous Environment Contamination and Its Control with Application to the Cryogenic Limb-Scanning Interferometer Radiometer (CLIR)		5. Report Date May 1979	
		6. Performing Organization Code 420	
7. Author(s) John J. Scialdone		8. Performing Organization Report No. G-5500	
9. Performing Organization Name and Address  Goddard Space Flight Center Greenbelt, Maryland 20771		10. Work Unit No.	
		11. Contract or Grant No.	
12. Sponsoring Agency Name and Address  National Aeronautics and Space Administration Washington, D.C. 20546		13. Type of Report and Period Covered  Technical Memorandum	
		14. Sponsoring Agency Code	
15. Supplementary Notes			
16. Abstract  A prediction of the in-orbit gaseous environment and the contamination it could produce on cryogenic and room temperature surfaces of payloads in the shuttle bay has been carried out. The time-varying environment was obtained by the superposition of the calculated shuttle environment for a discrete time and payload induced environments measured in large space chambers. The payloads will dictate the environment with the exception of periods when the attitude motors and water-release operations are in operation. Representative contaminant surface accretions have been calculated for flights 1 week and 1 month long for payloads having the largest source of outgassing and an orbit of 200 km. Based on the magnitude of the sources, their molecular natures, the decay rate with time, the sticking coefficients, the view factors, and the temperatures of the surfaces being contaminated, a number of calculations were made. These calculations led to a number of results. On direct viewing surfaces at less than 130 K, the contaminant accumulation could be about $10^{-2}$ cm for a 1-week flight and 10 percent more for a 1-month flight. The same surfaces at normal temperatures may acquire an early accumulation of about $10^{-5}$ cm of non-volatile residue materials. However, this deposit will leave the surfaces slowly, and, at the end of 1 week, its thickness should be $10^{-8}$ - $10^{-9}$ cm. The recommended observation column densities of less than $10^{12}$ cm <sup>-2</sup> will be attained later than 10 hours into the flight, depending on the onboard payloads. The attitude motors and evaporators will induce columns of $10^{14}$ - $10^{15}$ cm <sup>-2</sup> during their operations. At a surface temperature of <150 K, they will deposit on directly exposed surfaces at a rate of $10^{-8}$ - $10^{-9}$ cm/s. This will result from scattering at 200 km. A nonvolatile fraction of the motor products may accrete at a rate of $10^{-9}$ cm/s on a surface that is at room temperature. The natural oxygen at 200-km can accrete on a surface at less than 35-K at a maximum rate of $7 \times 10^{-8}$ cm/s. To reduce the contamination hazards, investigations have been performed on delaying the exposure of critical surfaces, on the effect of using vented helium as a counterflow to ingested oxygen in telescopes, on the effect of varying sublimation temperatures and times on the removal of condensed oxygen, and on the waiting time for normalization of the environment after operation of the control motors and/or evaporator. This document concludes with a list of precautions that can be taken during the design and operational phases of an instrument to limit the contamination to acceptable levels for short-duration Spacelab flights.			
17. Key Words (Selected by Author(s))  Shuttle/spacecraft, contamination, outgassing, condensation, adsorption, gaseous environment, contamination control		18. Distribution Statement  STAR Category 15 Unclassified-Unlimited	
19. Security Classif. (of this report)  Unclassified	20. Security Classif. (of this page)  Unclassified	21. No. of Pages  50	22. Price*  \$4.50



ASSESSMENT OF SHUTTLE PAYLOADS  
GASEOUS ENVIRONMENT CONTAMINATION AND ITS CONTROL  
WITH APPLICATION TO THE CRYOGENIC LIMB-SCANNING  
INTERFEROMETER RADIOMETER (CLIR)

John J. Scialdone

May 1979

GODDARD SPACE FLIGHT CENTER  
Greenbelt, Maryland 20771

All measurement values are expressed in the International System of Units (SI) in accordance with NASA Policy Directive 2220.4, paragraph 4.

## ABSTRACT

A prediction of the in-orbit gaseous environment and the contamination it could produce on cryogenic and room temperature surfaces of payloads in the shuttle bay has been carried out. The time-varying environment was obtained by the superposition of the calculated shuttle environment for a discrete time and payload induced environments measured in large space chambers. The payloads will dictate the environment with the exception of periods when the attitude motors and water-release operations are in operation. Representative contaminant surface accretions have been calculated for flights 1 week and 1 month long for payloads having the largest source of outgassing and an orbit of 200 km. Based on the magnitude of the sources, their molecular natures, the decay rate with time, the sticking coefficients, the view factors, and the temperatures of the surfaces being contaminated, a number of calculations were made. These calculations led to a number of results. On direct viewing surfaces at less than 130 K, the contaminant accumulation could be about  $10^{-2}$  cm for a 1-week flight and 10 percent more for a 1-month flight. The same surfaces at normal temperatures may acquire an early accumulation of about  $10^{-5}$  cm of non-volatile residue materials. However, this deposit will leave the surfaces slowly, and, at the end of 1 week, its thickness should be  $10^{-8}$ - $10^{-9}$  cm. The recommended observation column densities of less than  $10^{12}$  cm<sup>-2</sup> will be attained later than 10 hours into the flight, depending on the onboard payloads. The attitude motors and evaporators will induce columns of  $10^{14}$ - $10^{15}$  cm<sup>-2</sup> during their operations. At a surface temperature of <150 K, they will deposit on directly exposed surfaces at a rate of  $10^{-8}$ - $10^{-9}$  cm/s. This will result from scattering at 200 km. A nonvolatile fraction of the motor products may accrete at a rate of  $10^{-9}$  cm/s on a surface that is at room temperature. The natural oxygen at 200-km can accrete on a surface at less than 35-K at a maximum rate of  $7 \times 10^{-8}$  cm/s. To reduce the contamination hazards, investigations have been performed on delaying the exposure of critical surfaces, on the effect of using vented helium as a counterflow to ingested oxygen in telescopes, on the effect of varying sublimation temperatures and times on the removal of condensed oxygen, and on the waiting time for normalization of the environment after operation of the control motors and/or evaporator. This document concludes with a list of precautions that can be taken during the design and operational phases of an instrument to limit the contamination to acceptable levels for short-duration Spacelab flights.





## CONTENTS

	<i>Page</i>
ABSTRACT .....	iii
INTRODUCTION .....	1
CONTAMINATION CRITERIA .....	2
SHUTTLE-INDUCED ENVIRONMENT DATA .....	3
SATELLITE-INDUCED ENVIRONMENT DATA .....	9
SHUTTLE OUTGASSING TIME DEPENDENCE .....	14
PAYLOADS REPRESENTATION .....	14
EVALUATION OF THE SHUTTLE PAYLOAD ENVIRONMENT PARAMETERS .....	15
SHUTTLE PAYLOAD COMBINED ENVIRONMENT .....	16
Density .....	16
Column Densities .....	16
Direct Fluxes .....	19
Return Fluxes .....	19
SURFACE CONTAMINATION .....	22
THEORY .....	22
PREDICTED CONTAMINANT DEPOSITS ON SHUTTLE PAYLOADS SURFACES .....	26
Early Stages of Flight .....	26
Outgassing Deposits on Cryogenic Surfaces .....	31
Deposit Rates of VCS and Evaporator Products .....	32
Oxygen Deposits on Cryosurfaces .....	32
METHODS FOR REDUCING CONTAMINATION .....	33
Gaseous Purging .....	33
Sublimation of Condensed Oxygen .....	34
Waiting Time After VCS and Evaporator Operation .....	35
DESIGN AND OPERATIONAL CONTAMINATION CONTROL .....	35

## CONTENTS (continued)

	<i>Page</i>
SUMMARY OF THE RESULTS .....	37
CONCLUSIONS .....	39

## ILLUSTRATIONS

<i>Figure</i>		<i>Page</i>
1	Shuttle configuration showing vent locations, sources of contamination, and lines of sight .....	4
2	Shuttle density versus distance at 400-km orbit .....	5
3	Shuttle column density versus LOS at 400-km orbit .....	6
4	Shuttle return flux versus LOS at 400-km orbit .....	7
5	Density, pressure, and flux ratios at the spacecraft surface, produced by outgassed molecules returning to the satellite (for $\lambda_0 > 21$ R) .....	8
6	Pressure and density produced by outgassing versus distance from the spacecraft surface .....	9
7	Polar flux, density, and pressure produced by the CTS at 1 m from its equivalent surface (equivalent orbit is 300 km) .....	10
8	IMP-H spacecraft outgassing flux, $\phi_0$ , versus time at its surface .....	12
9	Mass flux at 1 m from CTS and IMP-H spacecraft equivalent surface .....	13
10	Density versus time at 1 m for STS with payload .....	17
11	Column density versus time for STS with payload .....	18
12	Direct flux at 1 m versus time for STS with payload .....	20
13	Molecular return flux versus time and orbit for STS with payload .....	21
14	Time for maximum deposit of H <sub>2</sub> O and DC-705 oil on a surface at T(K) for flux decaying as $t^{-3/2}$ and having a value $\alpha\gamma\phi_{10}$ at 10 hours .....	26

## CONTENTS (continued)

<i>Figure</i>		<i>Page</i>
15	Fraction of full outgassing (deposit) versus time for source decaying as $t^{-3/2}$ . . . . .	27
16	Maximum molecular deposit on surface versus time for contaminant flux decaying as $t^{-3/2}$ and having a value $\alpha\gamma\phi_{10}$ at 10 hours . . . . .	28
17	Fraction of total contaminant remaining when surface is exposed or cooled down $t$ (hr) after mission starts . . . . .	29
18	Conversion data from the mass flux rate, $m$ , to the number flux rate, $N$ ( $1/\text{cm}^2\text{-sec}$ ) . . . . .	31

## TABLES

<i>Table</i>		<i>Page</i>
1	Estimated Satellite Gaseous Parameters . . . . .	12
2	Instrument Contamination Predictions for Shuttle with LMOP/CTS-M-Type Payload at 200-km Orbit . . . . .	30



# **ASSESSMENT OF SHUTTLE PAYLOADS GASEOUS ENVIRONMENT. CONTAMINATION AND ITS CONTROL WITH APPLICATION TO THE CRYOGENIC LIMB-SCANNING INTERFEROMETER RADIOMETER (CLIR)**

## **INTRODUCTION**

Instruments and payloads carried by the Space Transportation System (STS) will be in a different space environment than that of the present satellites. This environment can degrade the observations and the measurements of the sources of energy being monitored. The degradation can be caused by the intervening gaseous and particulate medium that exists between the source and the instrument or by the deposits of this medium on thermo-optical surfaces. The most affected surfaces are those at cryogenic temperatures. The deposits may change the radiative properties of the surfaces, induce loss of optical transmittance, and produce light scattering and false indications of sources. The environment of payloads in the STS is dictated by the STS propulsion, life-sustaining, and power-generating systems and by material outgassing and shedding of particulates.

A preliminary assessment of the induced and natural environment of the STS with payloads has been performed. Its magnitude, deposit on surfaces, and controllability have been investigated. A generalized approach has been used to develop these data so that it may be used in the design and planning of instruments and payloads. Case-by-case detailed analyses must be performed later, when measured data on the STS environment and the particular design of the payloads will be available.

In this document, the gaseous environment for a payload or payloads in the STS were derived by the superposition of the calculated self-induced environment of the STS and the induced environment of a number of spacecraft, measured in large vacuum chambers. The density, direct fluxes, and column densities of the Shuttle and payloads were derived as a function of time, orbital altitudes and lines of sight. The contributions of the STS evaporator and vernier-control systems (VCS) are included.

Deposits of these molecular sources on surfaces at room and cryogenic temperatures were calculated, with attention to contamination of telescopes and, in particular, to the proposed cryogenic limb interferometer radiometer (CLIR). However, the calculations and relative plots in this document are general and can be used for any payload if geometrical factors and surface temperatures are known. The times during which contaminant deposits are possible were obtained from the expected magnitude of the contaminant after 10 hours in orbit, modified by the geometrical view factor between the source and the surface, the surface temperature, and the nature of the contaminant. The maximum deposit and the time for its eventual disappearance were estimated. The effect of delay in the exposure of a surface to the contaminant was evaluated. A list of the expected contaminant deposits on surfaces with direct or limited view (CLIR instrument) of the contaminant is provided. The deposits are based on the most severe expected environment of a general class of

payloads in the STS at a 200-km altitude. The effect of surface temperatures, the nature of the contaminant ( $\text{H}_2\text{O}$  or DC-705 silicone oil), the flight duration (1 week to 1 month), and the delay in exposure time were considered. Deposit rates from the emissions of the VCS and evaporator and from the natural oxygen were calculated. Methods for reducing cryogenic surface contamination using He as a purging gas or temperatures required for subliming the deposits were investigated. Also, the time required for the environment to become acceptable after the emission from a source such as the VCS and the evaporator was considered. The estimated environment was compared with the criteria limits on the environment suggested by the scientific community for satisfactory measurements and observations. Finally, a number of suggestions for limiting contamination through design and operational control are included.

## CONTAMINATION CRITERIA

Early in the Shuttle program, the scientific community set certain mission objectives and recommendations regarding the induced molecular and particulate contaminant emanating from the Shuttle. Volume X of Reference 1 lists the maximum allowable induced environment levels or criteria, which were subsequently clarified and expanded by the Contamination Requirements and Development Group (CRDG). The criteria\* state that it is a design and operational goal for the Orbiter and Spacelab to control the environment within the following limits:

- Column density

$10^{11}$  to  $10^{12}$   $\text{cm}^{-2}$ ,  $\text{H}_2\text{O} + \text{CO}_2$   
 $10^{13}$   $\text{cm}^{-2}$ ,  $\text{O}_2 + \text{N}_2$   
 $10^{10}$   $\text{cm}^{-2}$ , other gases

- Particulate emission

$<1$  discernible particle per orbit entering a  $1.5 \times 10^{-5}$  steradian (sr) field-of-view along any line within 60 degrees of the Z-axis (discernible particle is  $5\mu$  diameter within 10 km,

- Molecular deposition

$<10^{-5}$   $\text{g}/\text{cm}^2/30$  days/ $2\pi$  sr on 300-K surface  
 $<10^{-7}$   $\text{g}/\text{cm}^2/30$  days/ $0.1$  sr on 300-K surface  
 $<10^{-5}$   $\text{g}/\text{cm}^2/30$  days/ $0.1$  sr on 20-K surface  
 $(10^{-5}$   $\text{g}/\text{cm}^2/30$  days  $\approx 10^{12}$  molecules/ $\text{cm}^2/\text{s}$  average flux)  
 $\approx 1$ -percent optical degradation in infrared through ultraviolet by condensibles

---

\*Contamination Requirements and Development Group, Marshall Space Flight Center, July 22, 1975.

- Background brightness

Continuous emissions or scattering not to exceed 20th magnitude/sec<sup>2</sup> in the ultraviolet (equivalent to  $10^{-12} B_{\odot}$  at  $\lambda = 360 \times 10^{-9}$  m).

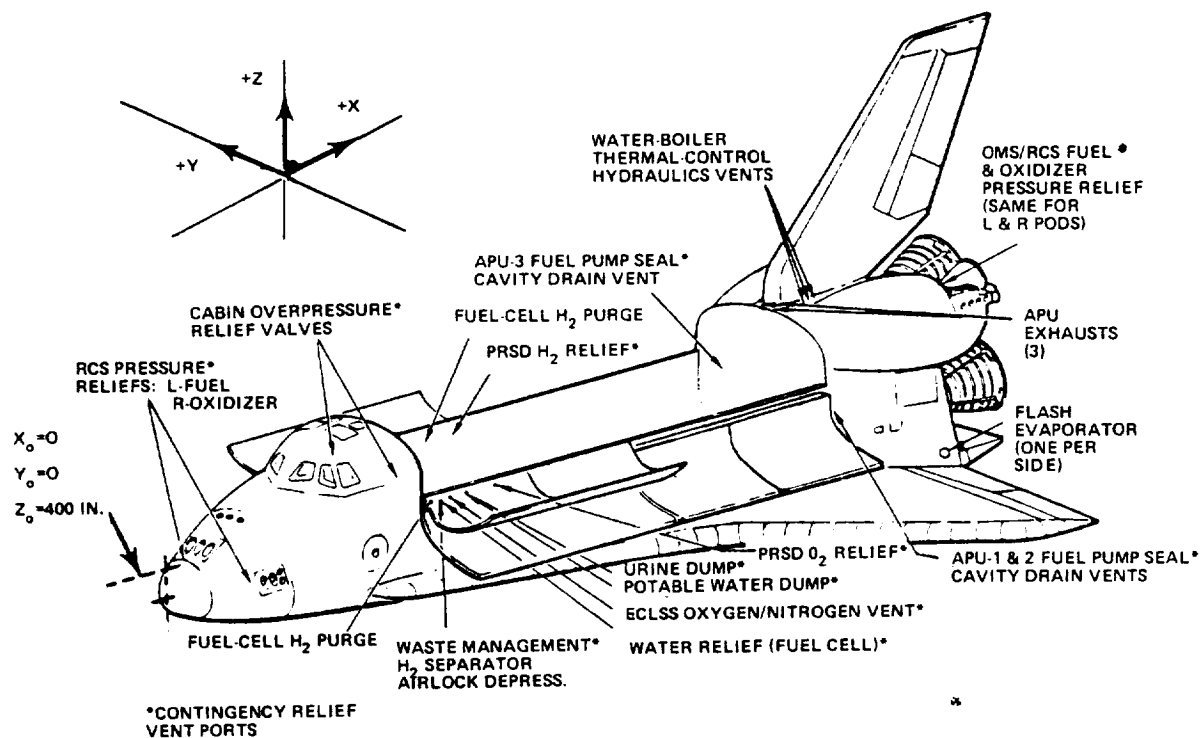
The Particle and Gas Contamination Panel (PGCP) has used these criteria as the basis for the contamination control of the Orbiter. This panel is implementing recommendations for design changes, material selections, contamination control, and flight and ground contamination monitoring.

## SHUTTLE-INDUCED ENVIRONMENT DATA

Figure 1 shows the Shuttle configuration with the vent locations and sources of contamination. Martin Marietta Aerospace and Johnson Space Center have used the Shuttle Payload Contamination Evaluation Program (SPACE) to model the Shuttle environment. Among other things, the model includes the geometries, the materials outgassing, and the various vent sources. It provides an estimate of the gaseous characteristic of the Shuttle and estimates of contaminant deposits on surfaces. Parameters of interest were calculated along lines of sight (LOS) identified in terms of the angles,  $\theta$  and  $\Phi$ , as shown in Figure 1. The origins of the LOS are at X=28.12 m, Y=0, Z=12.88 m. The data for the materials outgassing were obtained from previous experiences with the outgassing of the Skylab, from some tests on outgassing of sample materials, and by averaging the results of the 24-hour, 125°C volatile condensable material/total mass loss (VCM/TML) selection criteria tests on sample materials. Other sources, such as the evaporator, VCS, and cabin leak rates, were obtained from analytical estimates, tests, or previous experiences with similar systems.

The data for the plots in Figures 2, 3, and 4 were provided by the PGCP panel at Johnson Space Center or collected from References 2 and 3. These data were obtained using the Space Computer Program. Figure 2 shows the density versus distance for the Shuttle at a 400-km orbit. It shows that the densities produced by the evaporator and the VCS along LOS-1 and LOS-5 are maximum at about 10-15 m from the Shuttle origin. Their magnitudes,  $10^{-11}$  -  $10^{-12}$  g/cm<sup>3</sup>, are equal to pressures of about  $7 \times 10^{-6}$  to  $7 \times 10^{-8}$  torr. The maximum densities produced by material outgassing at maximum temperatures are  $8 \times 10^{-15}$  g/cm<sup>3</sup> ( $\sim 10^{-8}$  torr) for the early flight desorption and  $2.5 \times 10^{-15}$  g/cm<sup>3</sup> ( $\sim 10^{-9}$  torr) for outgassing beyond 10 hours in flight. The densities for low temperature conditions are also shown.

Figure 3 shows the column densities along various LOS for the Shuttle at a 400-km orbit produced by the same sources as before. These column densities are the integrated values of the density in a column 1 cm<sup>2</sup> of area from the surface of the Shuttle to infinity. As shown, the columns for the VCS and evaporator are in the  $10^{14}$  cm<sup>-2</sup> range, which are higher than the  $10^{12}$  cm<sup>-2</sup> columns considered acceptable. The plot shows that the columns produced by the materials outgassing of the Shuttle meet the criteria for the chosen conditions. Figure 4 shows the return fluxes of the several sources produced by their scattering with residual ambient molecules at 400-km. These molecules may condense or adsorb on the surfaces on which they impinge if the conditions of temperature



Line of Sight Number Designators

No.	$\theta$	$\Phi$	No.	$\theta$	$\Phi$
1	0	0	14	30	270
2	30	0	15	60	270
3	60	0	16	30	315
4	30	45	17	60	315
5	60	45	18	82.5	0
6	30	90	19	82.5	45
7	60	90	20	82.5	90
8	30	135	21	82.5	135
9	60	135	22	82.5	180
10	30	180	23	82.5	225
11	60	180	24	82.5	270
12	30	225	25	82.5	315
13	60	225			

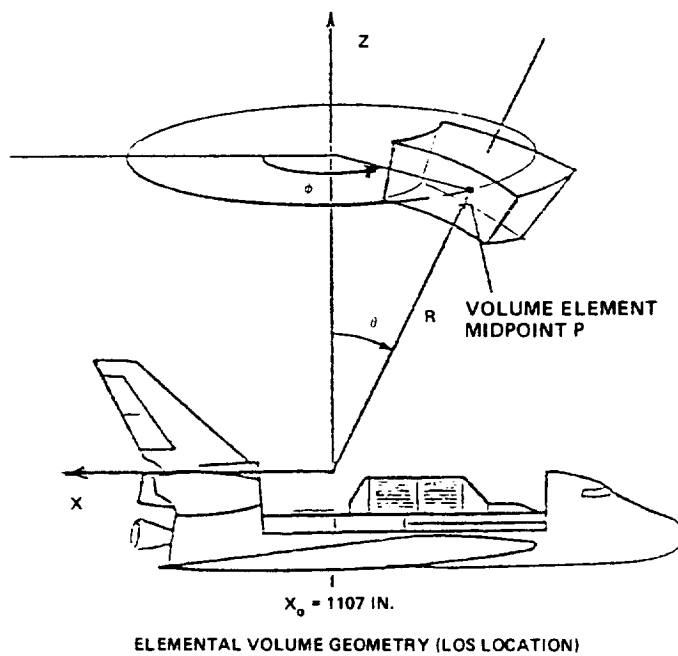


Figure 1. Shuttle configuration showing vent locations, sources of contamination, and lines of sight.



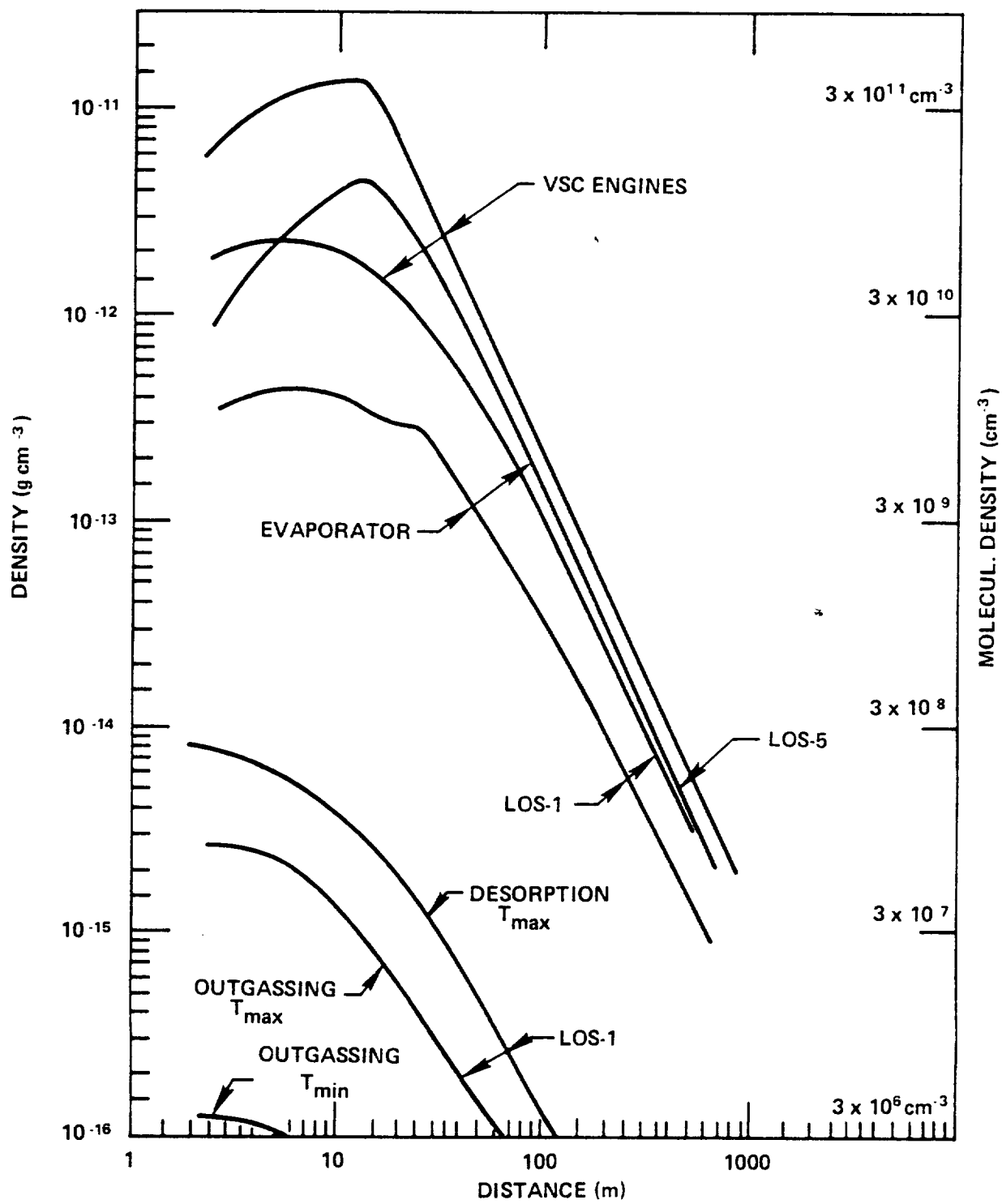


Figure 2. Shuttle density versus distance at 400-km orbit.

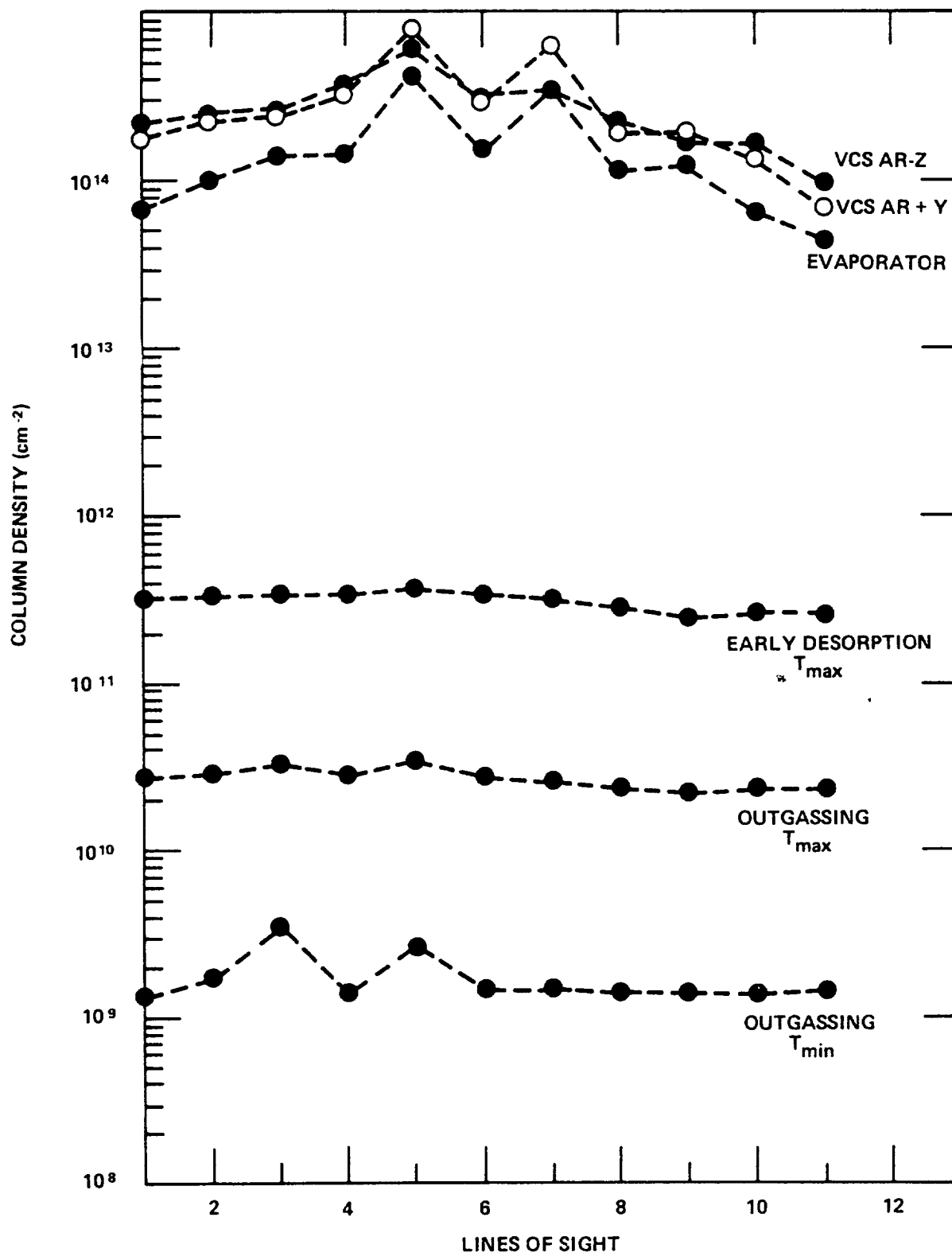


Figure 3. Shuttle column density versus LOS at 400-km orbit.

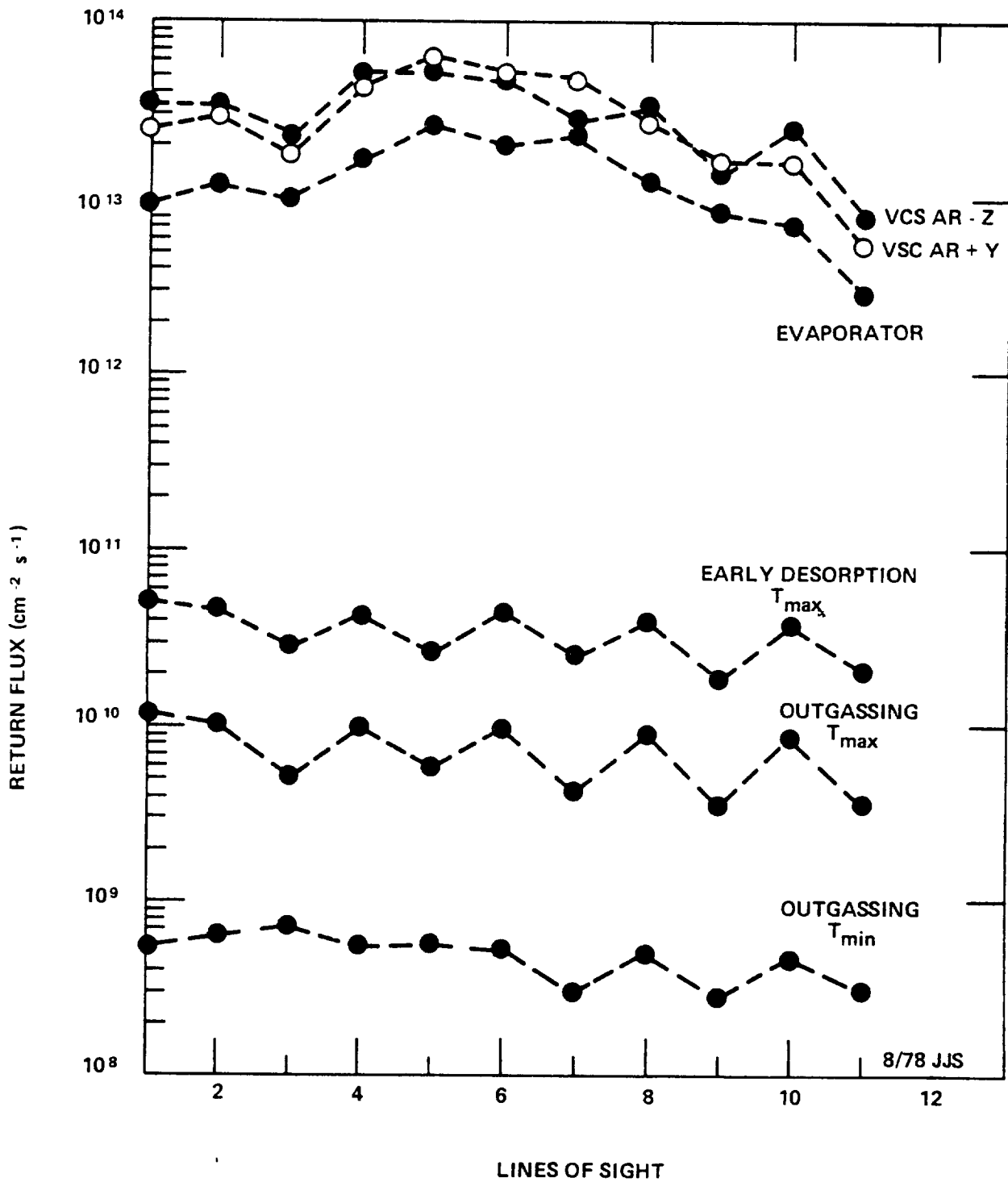


Figure 4. Shuttle return flux versus LOS at 400-km orbit.

favorable. The return fluxes at this altitude are approximately 1/32 of the returns expected at 200 km. Figure 4 shows that the return fluxes of the evaporator and VCS are about 3 orders of magnitude higher than those produced by the outgassing.

The data shown in these Figures 2, 3, and 4 apply to a 400-km orbit. For lower orbits, the return fluxes caused by ambient scattering will increase as shown in Figure 5 (Reference 4). At 300 km, the return is approximately 4 times larger than at 400 km, and, at 200 km, the return is about 32 times larger for the assumed source radii of 1 m or more. At these altitudes, the ambient scatter predominates over the self-scattering of the sources, which may become important at altitudes higher than 400 km. The density and column density are not affected by altitude being a function of the source strengths. However, as shown in Figure 6, their distributions with distance change. For orbits higher than about 200 km, the density is quasi-constant for about 1 m from the source. On the other end, for altitudes near 100 km, the density drops rapidly beyond 10 to 15 cm. These considerations could be helpful for instruments such as a telescope or probe. Moving out the entrance of the instrument 10 to 15 cm could provide much lower densities at the entrance when operating at lower orbits.

The molecular compositions of the sources from the Shuttle and payloads are estimated as follows. Early desorption from materials may consist of about 60-percent  $H_2O$ , 25-percent  $H_2$ , 10-percent  $CO_2$ , and the rest  $O_2$  and other molecules. Long-term outgassing will consist almost entirely of unreacted monomers and polymer chain fragments. The average molecular mass may be about 100-g/mole. The evaporator source is entirely water. The VCS and the reaction-control system (RCS) sources will consist of about 30-percent  $H_2O$ , 30-percent  $N_2$ , 10-percent  $CO$ , 20-percent  $H_2$ , and the rest  $O$ ,  $NO$ ,  $H_2$ , and some nonvolatile materials. (Although it is not shown in the plots, the RCS induces magnitudes 100 times or more than the VCS.)

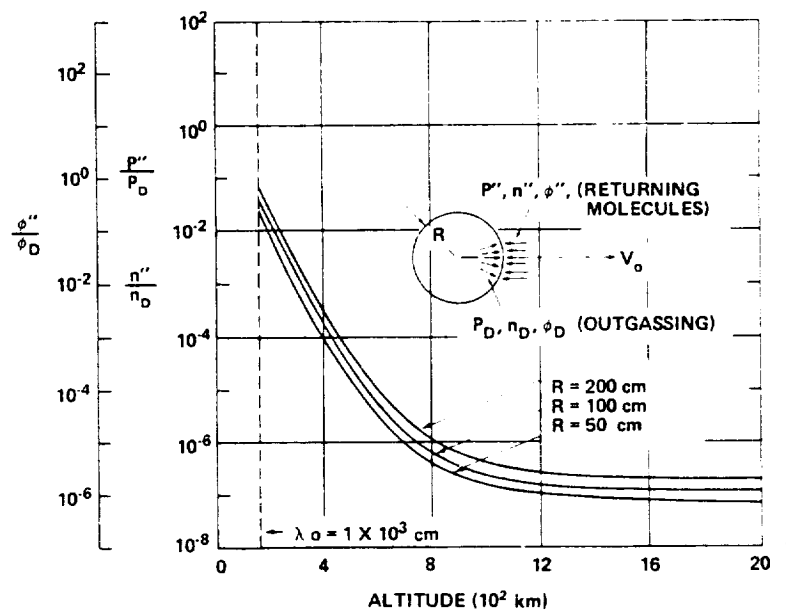


Figure 5. Density, pressure, and flux ratios at the spacecraft surface, produced by outgassed molecules returning to the satellite (for  $\lambda_0 > 21 R$ ).

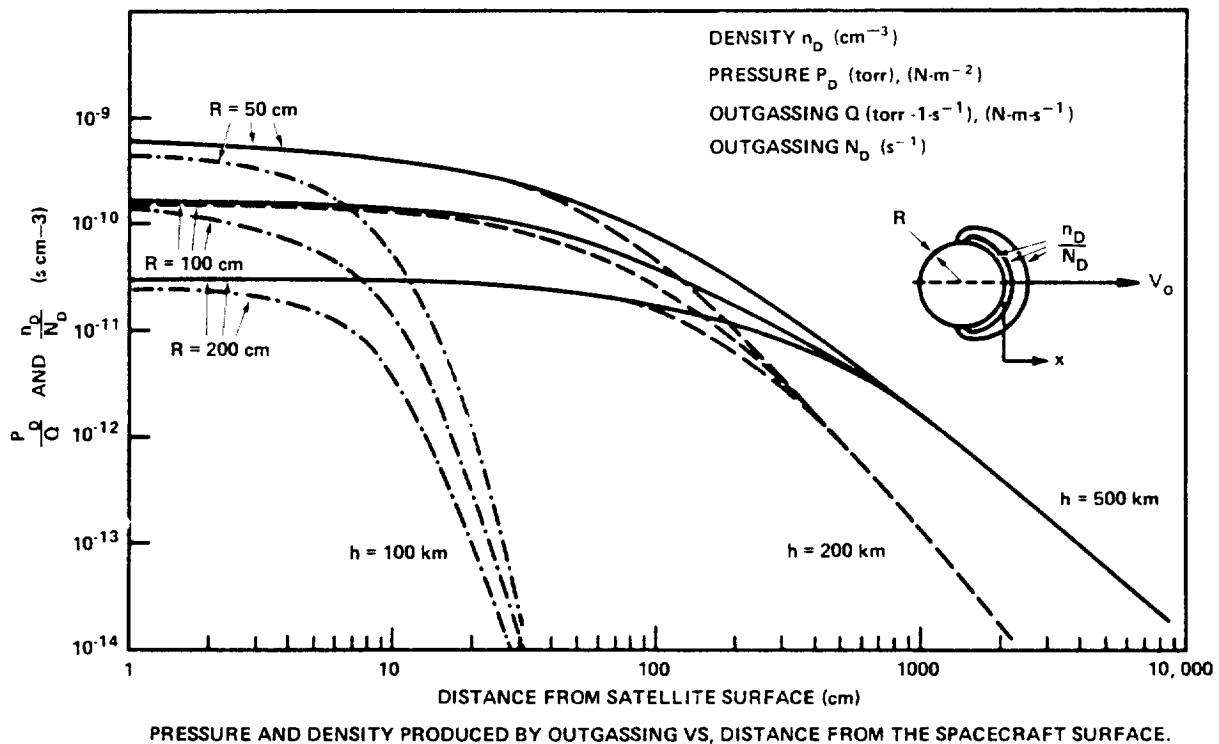


Figure 6. Pressure and density produced by outgassing versus distance from the spacecraft surface.

## SATELLITE-INDUCED ENVIRONMENT DATA

Payloads carried by the Shuttle will be exposed to the environment created by themselves and the Shuttle. The molecular and particulate environments produced by the payloads are not known at this time. They cannot be evaluated until data on the payload designs, missions, functions, etc., are known. Calculations similar to those performed for the Shuttle will be needed. Some specific estimates of the global environment have been made for the Shuttle with the Spacelab and with Defense Support Satellite (References 5 and 6). These estimates are based on conditions that exist during certain periods of the flights and some assumptions on the magnitudes of the outgassing sources. In this document data from past experience on satellite-induced environments are used to generate generalized payload environments. These environments, together with that estimated for the Shuttle, can provide expected global environments for future payloads.

The author obtained data on spacecraft-induced environments from tests in large vacuum chambers. Measurements were made on the Canadian Technology Satellite (CTS), the Interplanetary Monitoring Platform (IMP-H) and the Atmospheric Explorer D (AE-D). The CTS weight was 340 kg, and its configuration could be assumed to have an equivalent spherical radius of 1.37 m. The IMP-H weighed about 260 kg and approached a cylinder 1.57 m long with a 1.6-m diameter. The AE-D satellite weighed 679 kg and approximated a cylinder 1.14 m long with a 1.36-m diameter. Figure 7 shows the polar flux, density, and equivalent pressure at 1-m distance and in a plane through the

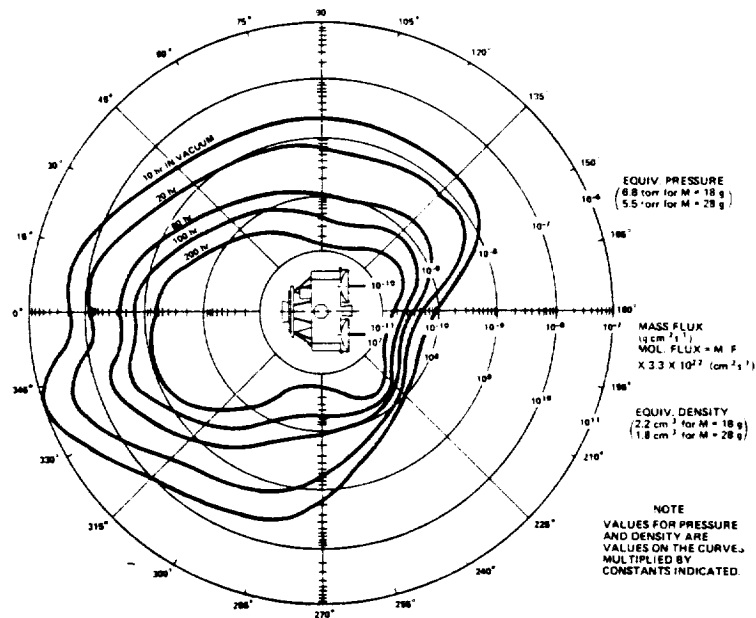


Figure 7. Polar flux, density, and pressure produced by the CTS at 1 m from its equivalent surface (equivalent orbit is 300 km).

CTS (Reference 7). These parameters were measured as a function of time with two back-to-back mounted quartz crystal microbalances (QCM), cooled at  $\text{LN}_2$  temperature. From geometrical considerations and chamber temperatures, the test simulated the outgassing conditions of the spacecraft when orbiting at 300 km. Figure 8, taken from Reference 8, shows test results with the IMP inside the same large chamber. In this case, the integrated outgassing flux versus time was obtained with the two back-to-back mounted tubulated ion gages while the spacecraft was slowly rotating. Mass spectrometer measurements during these tests indicated that the outgassing consisted of about 90-percent condensibles,  $M < 44$  g/mole, during the first 10 to 20 hours. Later, the condensibles were about 50-percent of the outgassing, and there was an increasing fraction of larger molecular-weight products. Complementary information on spacecraft outgassing was obtained from tests on the AE-C (Reference 9) and from data such as those listed in Table 1 (Reference 4).

Figure 9 shows the measured changes in outgassing rates as a function of time and angular positions from the CTS test. The measurements were taken for a period of about 150 hours, beginning after the spacecraft had been in the chamber for about 10 hours. Most of the outgassing curves in this plot show a decay with time according to a  $t^{-1.5}$ - $t^{-1.8}$  law, with the exception of the angular positions at 190 and 235 degrees, which show a rate approaching a  $t^{-1/2}$  law. These laws reflect a diffusion-controlled outgassing process. In fact, the solution of the equation for diffusive outgassing of a slab of material is an exponential function of time that approaches a  $t^{-1/2}$  slope for an initial period of time and then changes to a slope whose asymptote is a  $t^{-3/2}$  curve (Reference 10). The time at which the two slopes intersect is dictated by the thickness and diffusion coefficient of the material. This would indicate that the outgassing at the two angular positions with the  $t^{-1/2}$  decay eventually decay like the others according to  $t^{-3/2}$ . In Figure 9, the total outgassing of

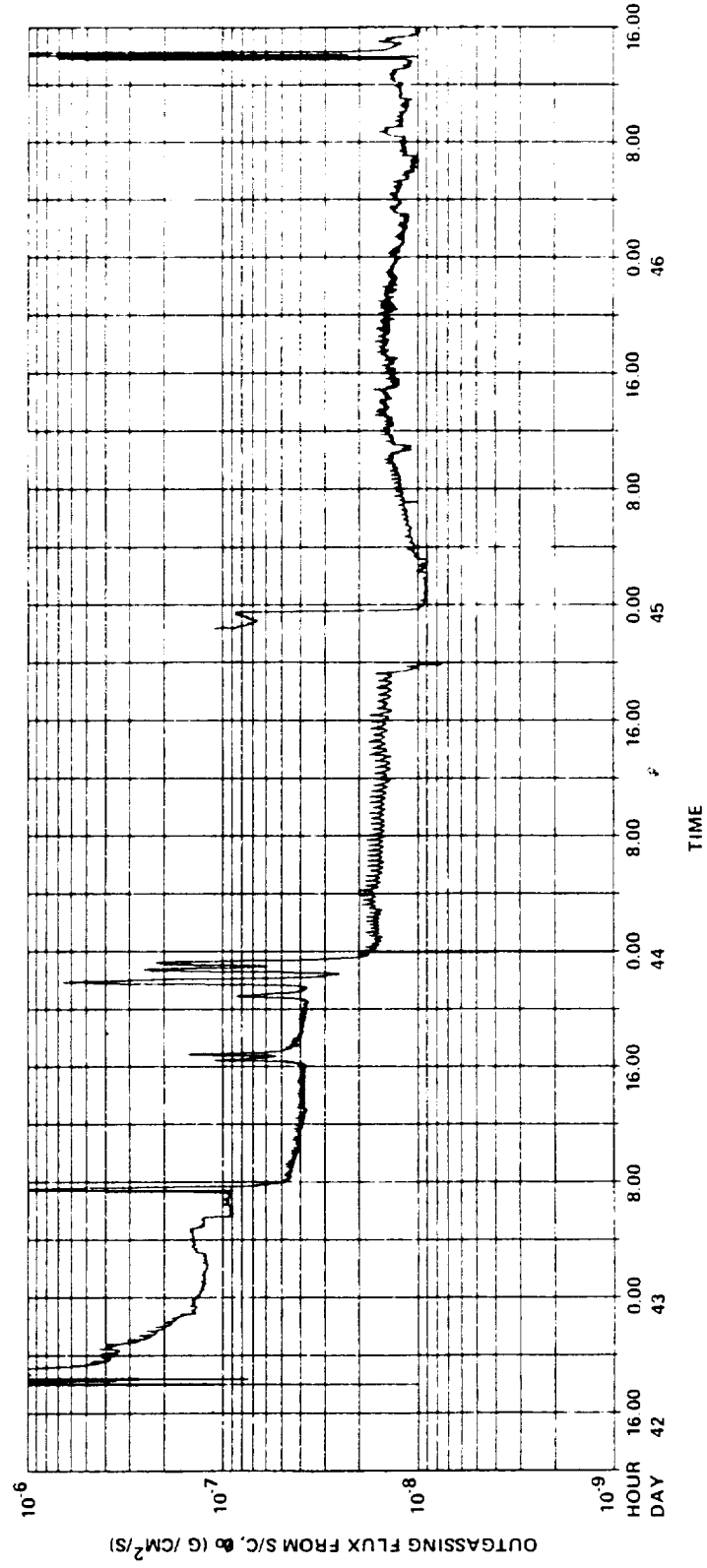


Figure 8. IMP-H spacecraft outgassing flux,  $\phi_0$ , versus time at its surface.

Table 1  
Estimated Satellite Gaseous Parameters

Satellite	Parameter					
	Satellite Radius- $R_E$ (cm)	Altitude-h (km)	Neutral Concentration- $n_0$ ( $\text{cm}^{-3}$ )	Pressure- $P_0$ (torr)	Mean Free Path- $\lambda_0$ (cm)	Outgassing (given/calculated)
						Q (torr- $\text{l-s}^{-1}$ ) m ( $\text{g-s}^{-1}$ ) N (molecules- $\text{s}^{-1}$ )
Gemini 3	200	160	$5.24 \times 10^{10}$	$4.13 \times 10^{-6}$	$2.5 \times 10^3$	$4.3 \times 10^0$ $4.2 \times 10^{-3}$ $1.42 \times 10^{20}$
Gemini 2	200	300	$1.72 \times 10^9$	$1.95 \times 10^{-7}$	$1 \times 10^5$	$1.43 \times 10^1$ $1.4 \times 10^{-2}$ $4.75 \times 10^{20}$
Apollo	200	300	$1.72 \times 10^9$	$1.95 \times 10^{-7}$	$1 \times 10^5$	$3.06 \times 10^1$ $3 \times 10^{-2}$ $1.01 \times 10^{21}$
ATM	300	400	$3.48 \times 10^8$	$3.98 \times 10^{-8}$	$1 \times 10^6$	$1.02 \times 10^2$ $1 \times 10^{-1}$ $3.3 \times 10^{21}$
IMP 2	~50	200	$1.5 \times 10^{10}$	$1.35 \times 10^{-6}$	$8 \times 10^3$	$2 \times 10^0$ $2 \times 10^{-3}$ $6.6 \times 10^{19}$
ISIS 1	~55	575	$4 \times 10^7$	$4 \times 10^{-9}$	$1 \times 10^7$	$9 \times 10^{-1}$ $9 \times 10^{-4}$ $3 \times 10^{19}$
Nimbus (FWS)	~70	1100	$9.45 \times 10^5$	$1.08 \times 10^{-10}$	$1 \times 10^9$	$8.9 \times 10^{-3}$ $8.9 \times 10^{-6}$ $2.8 \times 10^{17}$

## Calculations

Satellite	Parameter													
	Mean Free Path (cm)		Molecular Concentration (cm <sup>-3</sup> )			Pressure (torr)		Reverse Pressure P' (torr)	Flux (cm <sup>-2</sup> s <sup>-1</sup> )		Adsorption σ (cm <sup>2</sup> )	Condensation Rate ν (cm <sup>2</sup> s <sup>-1</sup> )	Time to form a Monolayer* t (s)	Mass Column Density M <sub>c</sub> (gm cm <sup>-2</sup> )
	Desorbed λ <sub>D</sub>	Reflected λ <sub>R</sub>	Reflected n <sub>R</sub>	Desorbed n <sub>D</sub>	Reverse n''	Reflected P <sub>R</sub>	Desorbed P <sub>D</sub>		Desorbed φ <sub>D</sub>	Reverse φ''				
Gemini 3	~1.0 × 10 <sup>2</sup>	6 × 10 <sup>2</sup>	7.95 × 10 <sup>10</sup>	7.1 × 10 <sup>9</sup>	~4.9 × 10 <sup>8</sup>	6.22 × 10 <sup>-6</sup>	2.15 × 10 <sup>-7</sup>	~1.5 × 10 <sup>-8</sup>	2.83 × 10 <sup>14</sup>	~1.96 × 10 <sup>14</sup>	~1.96 × 10 <sup>10</sup>	1.96 × 10 <sup>14</sup>	2.68	2 × 10 <sup>-12</sup> (6.6 × 10 <sup>10</sup> ) <sup>†</sup>
Gemini 2	5 × 10 <sup>3</sup>	3.5 × 10 <sup>4</sup>	2.6 × 10 <sup>9</sup>	2.83 × 10 <sup>10</sup>	1.13 × 10 <sup>8</sup>	2.94 × 10 <sup>-7</sup>	8.65 × 10 <sup>-7</sup>	3.45 × 10 <sup>-9</sup>	1.11 × 10 <sup>15</sup>	4.5 × 10 <sup>13</sup>	4.5 × 10 <sup>9</sup>	4.5 × 10 <sup>13</sup>	11.6	6.9 × 10 <sup>-12</sup>
Apollo	5 × 10 <sup>3</sup>	3.5 × 10 <sup>4</sup>	2.6 × 10 <sup>9</sup>	6 × 10 <sup>10</sup>	2.9 × 10 <sup>8</sup>	2.94 × 10 <sup>-7</sup>	1.84 × 10 <sup>-7</sup>	6.12 × 10 <sup>-9</sup>	2.4 × 10 <sup>15</sup>	9.6 × 10 <sup>13</sup>	9.6 × 10 <sup>9</sup>	9.6 × 10 <sup>13</sup>	5.5	1.4 × 10 <sup>-11</sup>
ATM	4.5 × 10 <sup>4</sup>	3 × 10 <sup>5</sup>	5.25 × 10 <sup>8</sup>	2.3 × 10 <sup>11</sup>	1.71 × 10 <sup>8</sup>	6 × 10 <sup>-8</sup>	7.14 × 10 <sup>-6</sup>	5.32 × 10 <sup>-9</sup>	9.25 × 10 <sup>15</sup>	5.5 × 10 <sup>13</sup>	5.5 × 10 <sup>9</sup>	5.5 × 10 <sup>13</sup>	9.6	3.2 × 10 <sup>-11</sup> (1 × 10 <sup>12</sup> ) <sup>†</sup>
IMP 2	4 × 10 <sup>2</sup>	2 × 10 <sup>3</sup>	2.25 × 10 <sup>10</sup>	5.26 × 10 <sup>10</sup>	6.6 × 10 <sup>8</sup>	2.03 × 10 <sup>-6</sup>	1.6 × 10 <sup>-6</sup>	2 × 10 <sup>-8</sup>	2.1 × 10 <sup>15</sup>	2.3 × 10 <sup>14</sup>	2.3 × 10 <sup>10</sup>	2.3 × 10 <sup>14</sup>	2.28	3.9 × 10 <sup>-12</sup> (1 × 10 <sup>11</sup> ) <sup>†</sup>
ISIS 1	5.5 × 10 <sup>5</sup>	4 × 10 <sup>6</sup>	6 × 10 <sup>7</sup>	2.4 × 10 <sup>10</sup>	1.55 × 10 <sup>5</sup>	6 × 10 <sup>-9</sup>	7.2 × 10 <sup>-7</sup>	4.66 × 10 <sup>-13</sup>	9.7 × 10 <sup>14</sup>	5.8 × 10 <sup>10</sup>	5.8 × 10 <sup>6</sup>	5.8 × 10 <sup>10</sup>	9.15 × 10 <sup>3</sup>	1.6 × 10 <sup>-12</sup>
Nimbus	6.5 × 10 <sup>7</sup>	4 × 10 <sup>8</sup>	1.4 × 10 <sup>6</sup>	1.68 × 10 <sup>8</sup>	1.6 × 10 <sup>1</sup>	1.62 × 10 <sup>-10</sup>	5.3 × 10 <sup>-9</sup>	5.3 × 10 <sup>-16</sup>	6.75 × 10 <sup>12</sup>	1.68 × 10 <sup>7</sup>	1.68 × 10 <sup>3</sup>	P' < P	3.12 × 10 <sup>17</sup>	1.3 × 10 <sup>-14</sup>

\*A monolayer of  $\text{H}_2\text{O}$ ,  $5.27 \times 10^{14}$  molecules  $\text{cm}^{-2}$

<sup>†</sup>Number column density expressed in  $\text{cm}^{-2}$



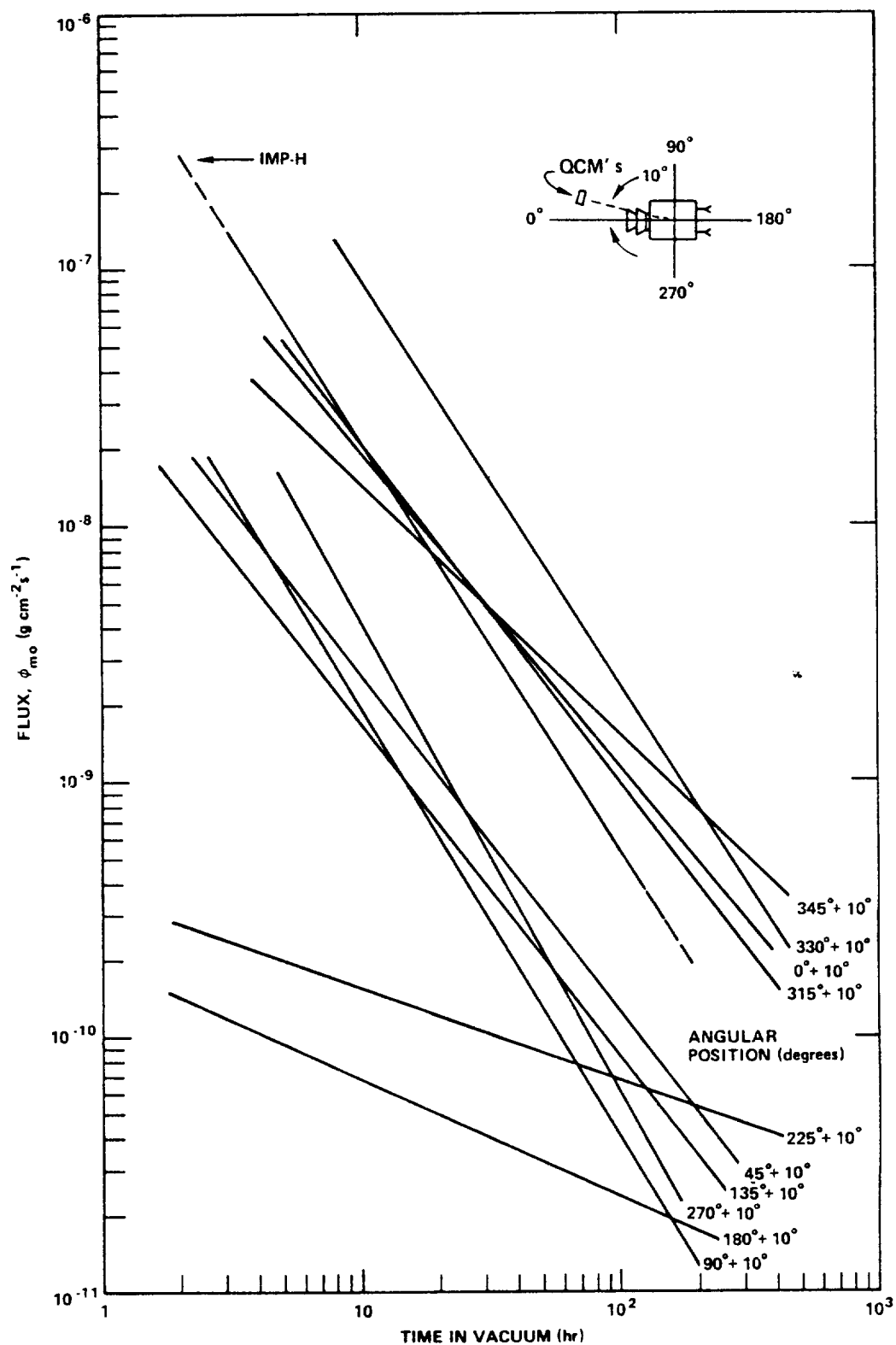


Figure 9. Mass flux at 1 m from CTS and IMP-H spacecraft equivalent surface.

IMP-H shown in Figure 8 has been superposed on the outgassing rates of the CTS and its outgassing decay also shows a similar time dependence. The outgassing was not measured during the early hours of vacuum exposure because the large amount of outgassing at those times would rapidly saturate the measuring instruments. The early outgassing consists mainly of gases desorbed from the surfaces. This early outgassing decays rapidly to a much lower rate within 1 to 2 hours.

## SHUTTLE OUTGASSING TIME DEPENDENCE

Figures 2, 3, and 4 show the shuttle environment calculated for a 400-km orbit and at discrete times. The curve labeled "Early Desorption" is taken as the outgassing conditions that exist during the first 10 hours of flight, whereas the curve labeled "outgassing" appears to correspond to the outgassing conditions after 100 hours. In the absence of definite outgassing versus time definition of the Shuttle outgassing, it is suggested that its outgassing versus time may be similar to that of the CTS and IMP-H. There are some supportive arguments for this assumption. According to some results of outgassing measurements of the Skylab and the Orbiting Geophysical Observatory (OGO) reported in Reference 3 for the early hours of the flight, the outgassing could be represented by an exponential decaying function with a time constant of about 18 hours. This was followed by another exponential with a much longer time constant. For 100 hours, using the exponential with an 18-hour time constant, the drop in outgassing rate is comparable to the drop indicated by the  $3/2$  function. For a 10-hour span, the drop from the same exponential equals that given by the  $1/2$  function.

The long-term outgassing can be associated to a slow rate of degradation of the material. Another supportive argument to the assumption may be provided by recent tests (Reference 11) on the RTV 560 silicone rubber used extensively for thermal protection of the Shuttle. These tests showed that the outgassing of this material followed the classical diffusion-controlled process. In view of these considerations, it is assumed that the Shuttle outgassing decays similarly to that of the CTS and IMP-H (i.e., approximately with a  $t^{3/2}$  law). This decay should be valid for a period from sometime before 10 hours to a time at which this outgassing curve intersects the long-term outgassing. The magnitudes for "early desorption" will be assumed to exist at 10 hours. Regardless, it will be seen later that the total environment for the payloads will be dictated by their own outgassing.

## PAYLOADS REPRESENTATION

As mentioned, the Shuttle payload environment was obtained by combining the Shuttle data shown in Figures 2, 3, and 4 with the experimental data from the mentioned spacecraft. The Shuttle data for early desorption were taken to exist at 10 hours, and the outgassing was a long-term condition. The magnitudes were taken at a 1-m distance from the origin along LOS (lines of sights) showing maximum values. The IMP-H, which may simulate a scientific payload, and two configurations of the CTS technological satellite are representative payloads. One configuration is a CTS-Maximum (CTS-M) that represents a spacecraft that includes a spent solid motor with 10-hour outgassing rate corresponding to the maximum flux shown in Figure 7. The other, designated CTS-Average (CTS-A) and representing an average spacecraft of that type without a spent motor, has a flux at 10

hours that corresponds to the integrated average of that shown in Figure 7. Additional data on combined Shuttle payload environment were obtained from Reference 5, which provided predictions for early desorption and later outgassing of the STS with the long module one pallet (STS/LMOP) at 200- and 250-km orbits.

## EVALUATION OF THE SHUTTLE PAYLOAD ENVIRONMENT PARAMETERS

Data for the Shuttle at a 400-km orbit, for CTS and IMP-H at a 300-km orbit, and for the STS/LMOP at a 200- to 250-km orbit have been reevaluated for altitudes of 200, 300, and 400 km. The following established relationships have been used for each parameter.

The direct flux is given by

$$\phi_D = n V_D \quad (\text{cm}^{-2} \text{ s}^{-1}) \quad (1)$$

where  $n$  ( $\text{cm}^{-3}$ ) is the density, and

$$V_D = \sqrt{\frac{8RT}{\pi M}} = 1.45 \times 10^4 \sqrt{\frac{T}{M}} \quad (\text{cm s}^{-1})$$

is the mean outgassing velocity of the molecules of molecular mass,  $M$  (g/mole), and temperature,  $T$ (K).

The ambient scattered return fluxes,  $\phi_R$  ( $\text{cm}^{-2} \text{ s}^{-1}$ ), were obtained from References 4 and 12:

$$\frac{\phi_R}{\phi_D} = \frac{R}{\lambda_0} \left( \frac{V_s}{V_D} + 1 \right) \quad (2)$$

where  $R$  (cm) is the radius of the emitting source,  $\lambda_0$  (cm) is the ambient, mean-solar-activity, mean free path (Reference 13),  $V_D$  ( $\text{cm s}^{-1}$ ) is the mean outgassing molecular velocity, and  $v_s$  is the orbital velocity. This relationship appears in Figure 5.

The column density,  $N_C$  ( $\text{cm}^{-2}$ ), is approximated in Reference 12 by

$$N_C = \frac{\lambda_0}{V_s} \phi_R \sim \frac{\phi_D R}{V_D} \sim nR \quad (\text{cm}^{-2}) \quad (3)$$

The molecular self-scattering flux,  $\phi_{ss}$  ( $\text{cm}^{-2} \text{s}^{-1}$ ), which is complementary to the ambient scattering, was evaluated by using the approximate relation (Reference 12)

$$\phi_{ss} = \frac{1.78 \times 10^{-2}}{V_D} \sigma R \phi_D^2 \quad (\text{cm}^{-2} \text{s}^{-1}) \quad (4)$$

where  $\sigma$  ( $\text{cm}^2$ ) is the molecular cross section, and the other terms are the same as before.

## SHUTTLE PAYLOAD COMBINED ENVIRONMENT

The following paragraphs describe the predicted molecular environments of the Shuttle and of the Shuttle with representative payloads CTS-A, CTS-M, IMP, and LMOP with reference to Figures 10 through 13. The predicted parameters are density, column density, direct flux, and return fluxes.

### Density

As shown in Figure 10, the presence of payloads in the bay increases the density of the STS at 1 m by orders of magnitude. The density is dictated by the payloads until their rates of outgassing are the same as those of the STS. The calculated data for the STS and the STS plus the LMOP include a long-term density value. These have been incorporated and are shown on the respective density plots. The natural ambient densities at 200, 300, and 400 km are indicated for comparison.

Payloads similar to the CTS-M will induce densities equal to the ambient density at 300 km after 7 days in orbit. Those similar to the IMP and the CTS-A will have the same equivalent density after 50 to 60 hours and 15 to 20 hours, respectively. The STS/LMOP payload will be in a density equal to the 300-km natural density after many days. Note that the decay rates ( $\tau^{-3/2}$ ) used here are faster than the linear or square root decays that may also exist. Also, the presence in the bay of additional payloads with similar, same order magnitude outgassing will not significantly change these environments.

The densities that the VCS and the evaporator, which are maximum at about 12 m, induce from the bay, are also shown. These are always greater than those that the payloads produce with some exceptions during the early hours of the flight. However, the large densities will dissipate rapidly after the emissions stop, as will be discussed later. The densities along different lines of sight and different distances can be deduced from Figure 2.

### Column Densities

Figure 11 shows the column densities versus time that result from combining the Shuttle and payloads. Disregarding the molecular constituents of the columns, the criteria goal of the  $10^{12} \text{cm}^{-2}$   $\text{H}_2\text{O}$  column will be met within 10 hours with CTS-A, within 35 hours with the LMOP, within 10 hr

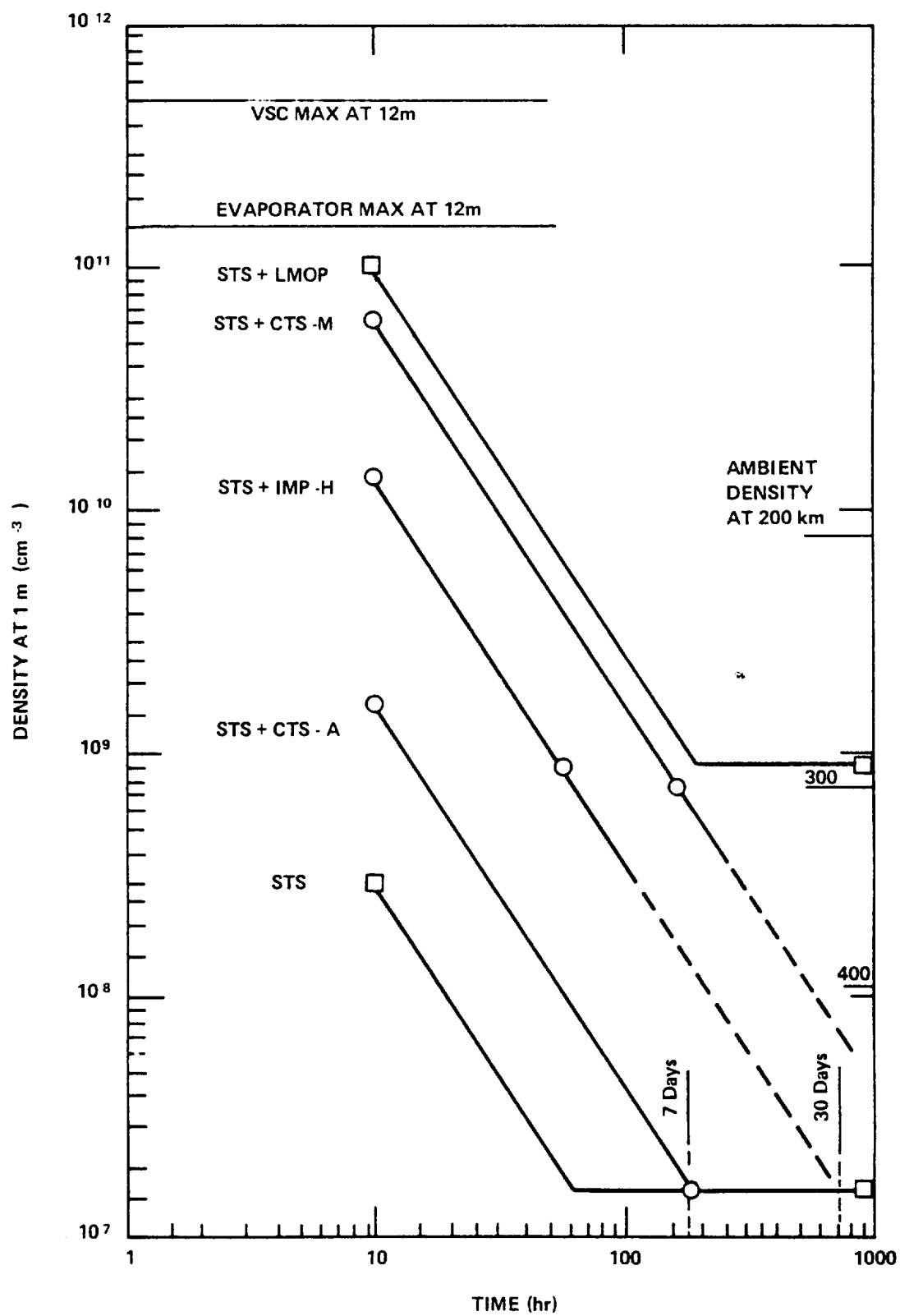


Figure 10. Density versus time at 1 m for STS with payload.

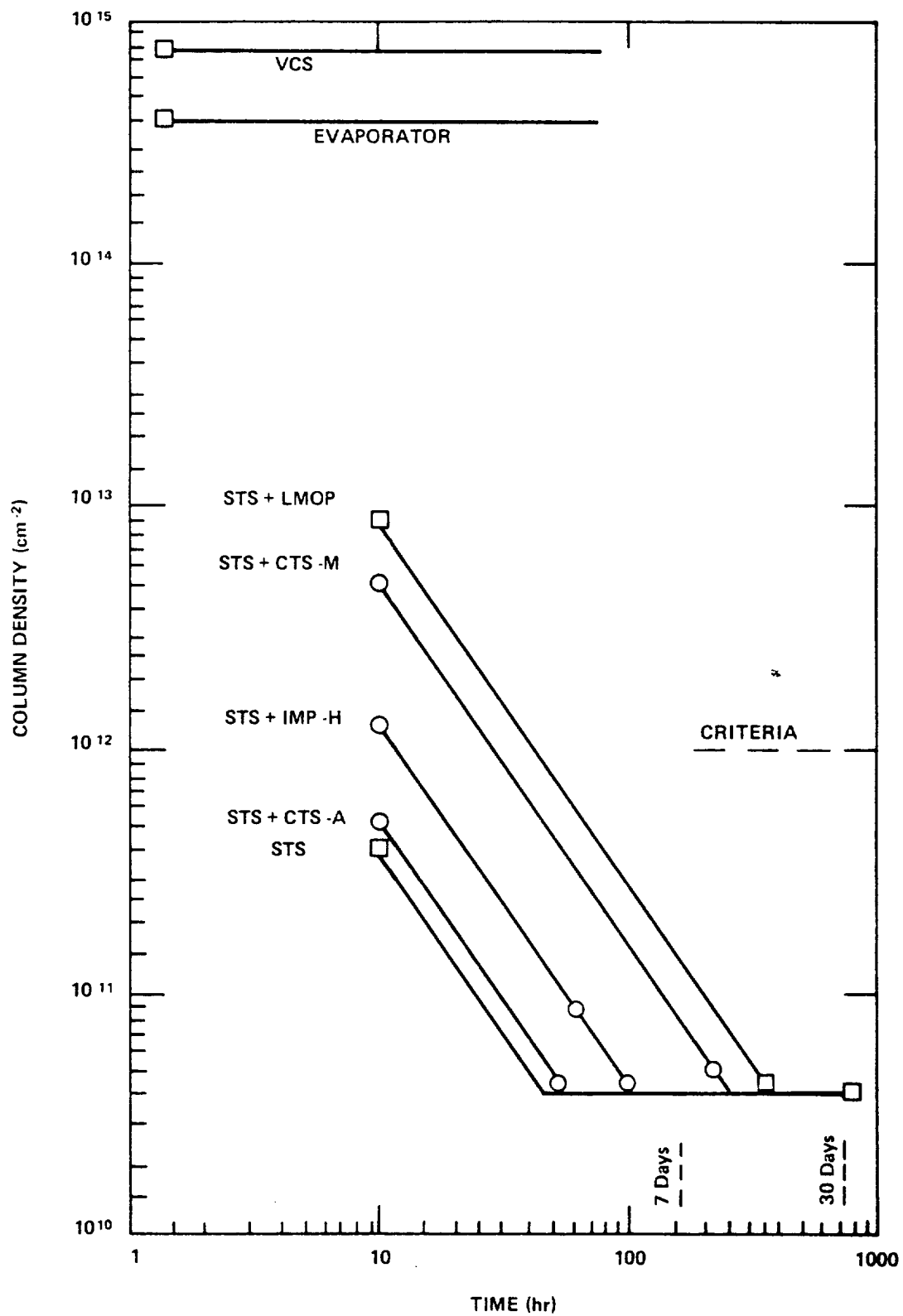


Figure 11. Column density versus time for STS with payload.

with IMP-H, and in about 30 hours for a payload with the CTS-M characteristics. However, the  $\text{H}_2\text{O}$  content of the column is estimated at about 60 percent after 10 hours in orbit and less than 10 percent thereafter. With this estimate, the criteria are met when the total column has a value of about  $10^{13} \text{ cm}^{-2}$ , which would exist for most of these payloads within 10 hours after launch. Although the columns produced by the VCS and evaporator are considerably higher than the criteria, they will exist only during their operations and for a few minutes thereafter.

### Direct Fluxes

Figure 12 shows the direct fluxes at 1 m that are produced by the STS and payloads. The fluxes for the STS and the STS/LMOP were calculated from the densities shown in Figure 2, using appropriate values for temperatures and molecular weight, and from the return fluxes and column densities given in Reference 5. The direct-flux calculations assume that the sources are from cylinders. The full reflection of the outgassing from the bay liner increases the fluxes by a factor of 2 without affecting the order of magnitude. These calculated fluxes, with data on view factors, nature of the constituents, and temperatures, can provide estimates of contamination risks on surfaces. For comparison, Figure 12 shows the flux that corresponds to a monolayer of  $\text{H}_2\text{O}$ . The monolayer flux will be established after 35 to 40 hours for the LMOP and CTS-M and after 10 to 12 hours for the IMP-H. Figure 12 also shows self-scattering magnitude of the flux from the STS/CTS-M. Its magnitude is about three orders of magnitude less than the direct flux and one order less than the ambient scatter at a 400-km orbit (Figure 13).

### Return Fluxes

In addition to the direct fluxes, return fluxes are produced from the scattering of the emitted molecules with the ambient molecules and particles. The return flux is a function of the source magnitude, of the molecule cross sections, and of the ambient density. It decreases with orbit altitudes and becomes quasi-constant at orbits above 600 to 700 km. Figure 13 shows the estimated returns on a  $2\pi$  surface for altitudes of 200, 300, and 400 km for the STS, for the STS with the payloads, and for the VCS and evaporator.

The recommended goal of a return flux not larger than  $10^{12} \text{ molecules/cm}^2$  (corresponding to  $\text{H}_2\text{O}$  accumulation of 1100 monolayers in 1 week) will be achieved for a 200-km orbit after 7 days by the Shuttle with the CTS-M, IMP-H, and LMOP and after about 40 hours for the Shuttle with the CTS-A. For a 300-km orbit,  $10^{12} \text{ cm}^{-2}$  is achieved after 60 hours by the IMP, after 140 hours by the CTS-M, and after 12 hours by the CTS-A. At 400 km, the criteria are achieved earlier. The STS alone achieves the criteria within 2 hours at 400 km and within 12 hours at 200 km. The STS/LMOP shows a long-term compliance with the criteria. The return from the VCS and evaporator will not meet this criteria at any of the altitudes considered. As indicated previously, the magnitude of self-scattering within the emitted flux of the STS/CTS-M was shown for convenience in the plot for the direct flux. It is about one order of magnitude less than the ambient return flux for this payload at a 400-km orbit.

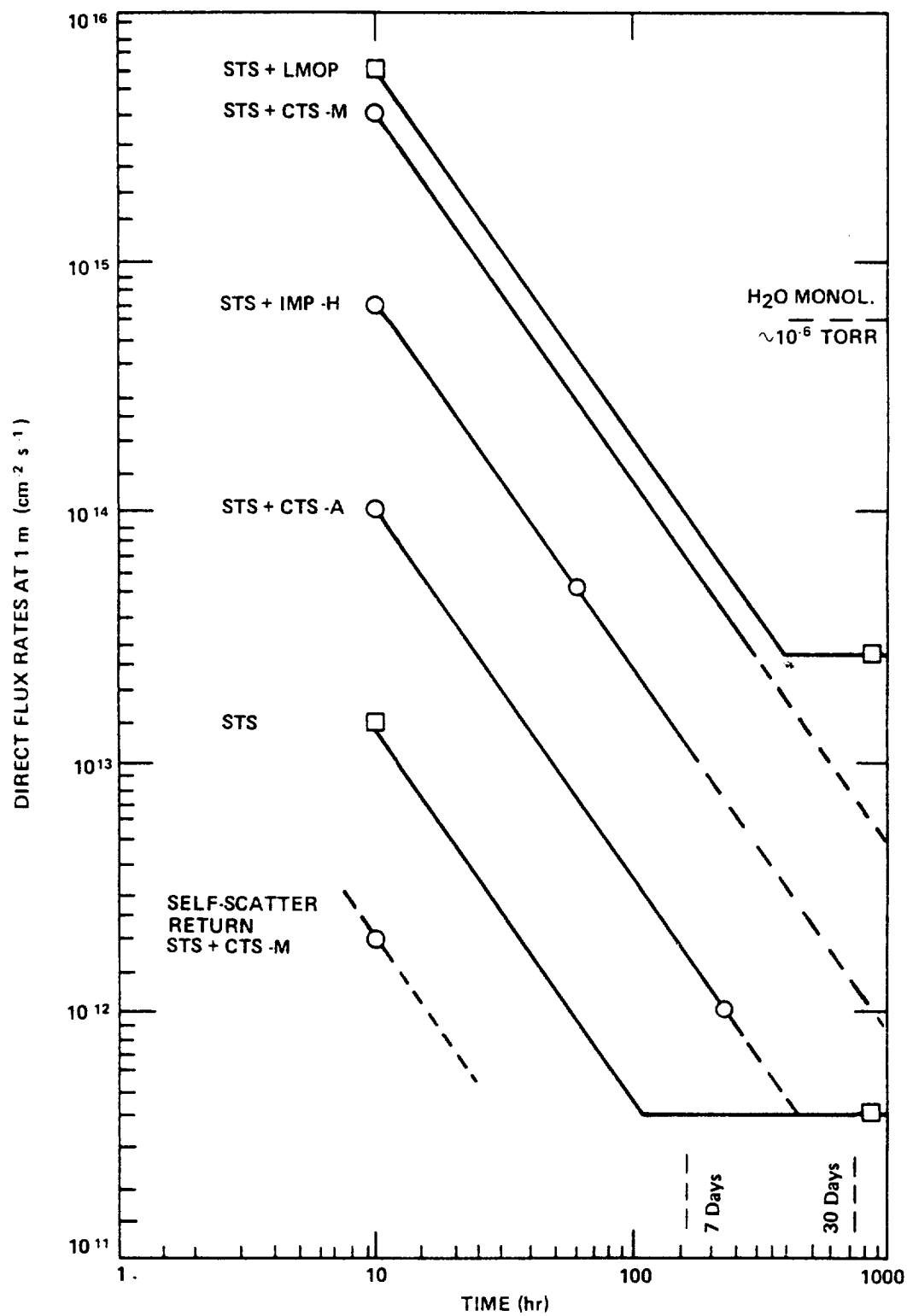


Figure 12. Direct flux at 1 m versus time for STS with payload.



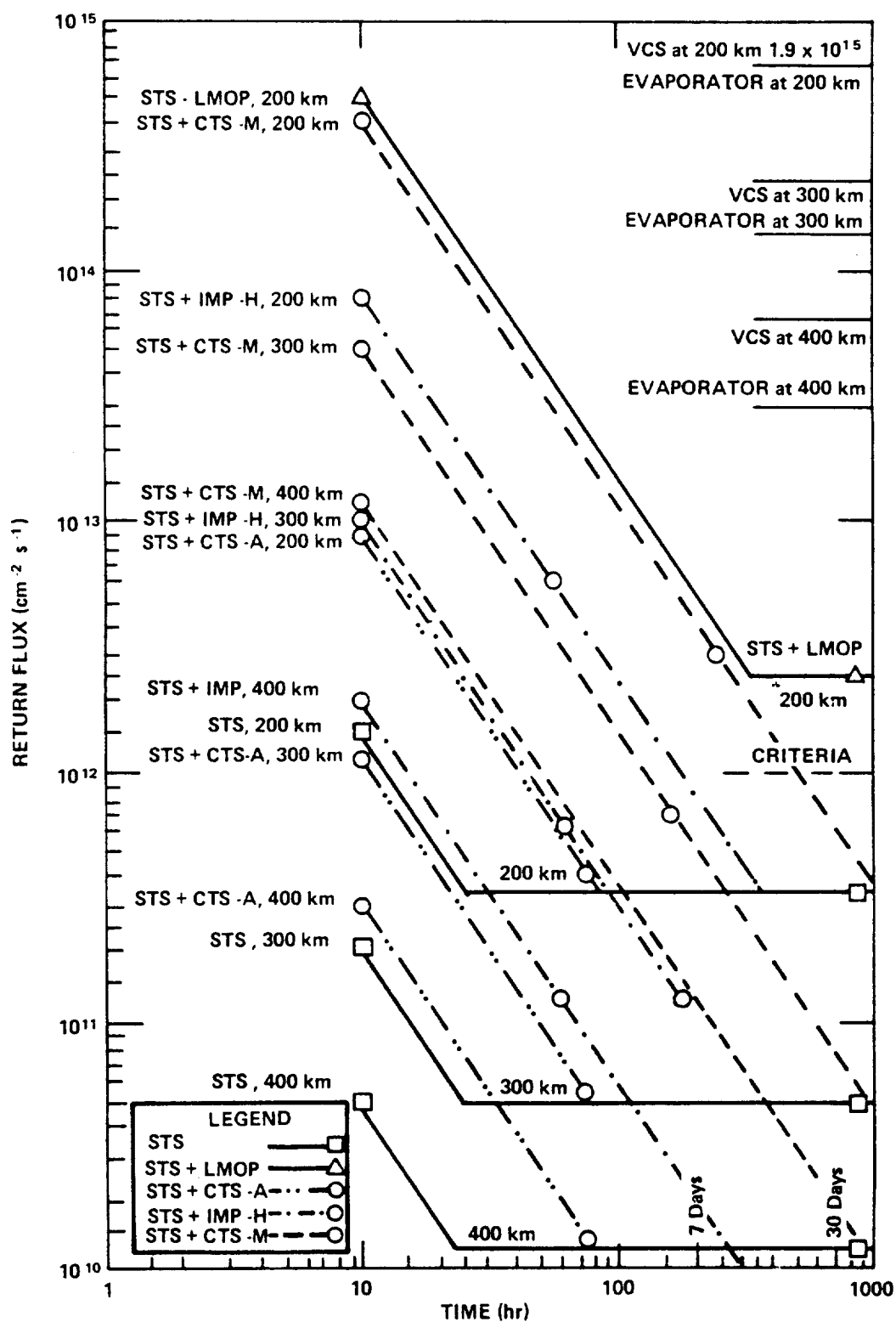


Figure 13. Molecular return flux versus time and orbit for STS with payload.

## SURFACE CONTAMINATION

The gaseous environment to which payloads in the Shuttle bay will be exposed (as derived in the previous pages) can be used to estimate contaminant deposits on critical surfaces. In addition to the source and the nature of its constituents, additional data are needed on the temperature of the surface and its geometrical view factor with respect to the source. The following paragraphs discuss contamination on surfaces in the bay that have direct or limited view of the source and are at normal or cryogenic temperatures. In particular, it discusses the probable contamination of CLIR (Reference 14), which has been proposed as an instrument to be carried on the Shuttle. CLIR includes a telescope with detectors at 10 K, a 25-cm diameter mirror at 30 K, and a baffle at 115 K. The view factor of the mirror is approximately  $6.2 \times 10^{-2}$ . However, before the deposits can be estimated, the tools for the calculations must be reviewed and developed.

Although the outgassing consists of many different molecules, the analysis and calculations for its deposit and reemission from surfaces has been carried out as if it were an equivalent single material. The contaminant source has been assumed to consist mainly of material having characteristics similar to water and to include some low vapor-pressure materials similar to the DC-705 silicone oil. This oil has an equivalent average vapor-pressure and activation energy.

## THEORY

The flux of contaminant impinging and sticking on a unit surface,  $\phi_i$ , is a function of the strength of the source, the view factor,  $\gamma$ , and the sticking (accommodations) factor,  $\alpha$ . For a variable source, it can be expressed as

$$\phi_i = \alpha \gamma \frac{\phi_{10} t_{10}^n}{t^n} \quad (\text{cm}^{-2} \text{ s}^{-1}) \quad (5)$$

where  $n$  is the exponent of the source decay function, which has a magnitude of  $\phi_{10}$  ( $\text{cm}^{-2} \text{ s}^{-1}$ ) at time  $t_{10}$  (s). The subscripts "10" in these two terms indicate that reference values at 10 hours have been chosen. Any other set of values could have been used. The sticking coefficient,  $\alpha$ , is close to 1 for the sources and surface temperatures under considerations. Reference 15 contains a list of its values. The flux of contaminant that leaves the surface,  $\phi_L$ , can be expressed in different forms, depending on whether it is a sublimation (evaporation) or a surface desorption process. For an evaporation, it is given by the Langmuir expression,

$$\phi_L = \frac{3.52 \times 10^{22}}{\sqrt{M T_s}} \beta P_s \quad (\text{cm}^{-2} \text{ s}^{-1}) \quad (6)$$

where  $\beta \sim 1$  is the evaporation coefficient,  $P_s$  (torr) and  $T_s$  (K) are the equivalent saturated vapor pressure and temperature of the material, molecular mass,  $M$  (g/mole), on the surface at  $T_s$ . In a desorption process, the flux is

$$\phi_L = \frac{N}{\tau_0} e^{-\frac{E}{RT_s}} \quad (\text{cm}^{-2} \text{ s}^{-1}) \quad (7)$$

where  $N(\text{cm}^{-2})$  is the number of molecules adsorbed on the unit surface,  $\tau_0 \sim 10^{-13}$  (s) is the oscillation period of the molecule on the surface at room temperature,  $E$  (cal/mole) is the activation or binding energy of the molecule on the surface (depending on the nature of the molecules and somewhat on the surface), and  $R$  (cal/mole/K) is the gas constant. The grouping,  $\tau = \tau_0 \exp E/RT$  (s), is the residence time of the molecule. An integration of the foregoing desorption flux equation gives the molecular density on the surface,  $\sigma$  ( $\text{cm}^{-2}$ ), as a function of time,  $t$ (s):

$$\sigma = \sigma_0 e^{-\frac{t}{\tau}} \quad (\text{cm}^{-2}) \quad (8)$$

where  $\sigma_0$  ( $\text{cm}^{-2}$ ) is the initial deposit density. Applying the conservation of mass, the rate of molecules accreting or leaving the surface per unit time is

$$\frac{dN_a}{dt} = \phi_i - \phi_L \quad (\text{cm}^{-2} \text{ s}^{-1}) \quad (9)$$

For condensation on the surface,  $\phi_i > \phi_L$ , and the relation for this case will be

$$\frac{dN_a}{dt} = \alpha \gamma \frac{(\phi_{i0} t_{i0}^n)}{t^n} - \frac{3.52 \times 10^{22}}{\sqrt{MT_s}} \beta P_s \quad (\text{cm}^{-2} \text{ s}^{-1}) \quad (10)$$

The accumulation reaches its maximum when  $dN_a/dt = 0$ . Thereafter, the second term,  $\phi_L$ , predominates, and the molecules leave the surfaces. The time,  $t_m$ , corresponding to maximum accumulation is

$$t_m = \left[ \alpha \gamma \phi_{i0} t_{i0}^n \right]^{1/n} \left[ \frac{\sqrt{MT_s}}{3.52 \times 10^{22} \beta P_s} \right]^{1/n} \quad (\text{s}) \quad (11)$$

Therefore, knowing the depositing material properties ( $P_s$ ,  $M$ ,  $T_s$ ) and the source intensity, one determines the time when accumulation stops and the contaminant begins to leave the surface (if not affected by radiation). The number of molecules,  $N$ , on the surface as a function of time can be found by integrating equation 10 between  $t_i$ , the time of initial exposure to the flux, and time  $t$ . The integration for positive values of  $n$  gives:

$$N = \alpha \gamma \phi_{10} t_{10}^n \int_{t_i}^t t^{-n} dt - \frac{3.52 \times 10^{22}}{\sqrt{MT_s}} \beta P_s (t - t_i) \quad (\text{cm}^{-2}) \quad (12)$$

For  $n < 1$ ,

$$N = \frac{\alpha \gamma \phi_{10} t_{10}^n}{1 - n} \left[ t^{1-n} - t_i^{1-n} \right] - \frac{3.52 \times 10^{22}}{\sqrt{MT_s}} \beta P_s (t - t_i) \quad (12a)$$

For  $n = 1$ ,

$$N = \alpha \gamma \phi_{10} t_{10}^n \ln \frac{t}{t_i} - \frac{3.52 \times 10^{22}}{\sqrt{MT_s}} \beta P_s (t - t_i) \quad (12b)$$

For  $n > 1$ ,

$$N = \frac{\alpha \gamma \phi_{10} t_{10}^n}{n - 1} \left[ t_i^{1-n} - t^{1-n} \right] - \frac{3.52 \times 10^{22}}{\sqrt{MT_s}} \beta P_s (t - t_i) \quad (12c)$$

Equation 12c is applicable to sources decaying as  $t^{-3/2}$ , which we have used in the description of the payloads environment. If the flux leaving the surface, as given by the Langmuir expression, is greater than the impinging flux, condensation cannot occur. However, a number of monolayers can form on the surface by virtue of short-range surface forces. The mass conservation in that case is

$$\frac{dN_a}{dt} = \frac{\alpha \gamma \phi_{10} t_{10}^n}{t^n} - \frac{N_{AD}}{\tau} \quad (\text{cm}^{-2} \text{ s}^{-1}) \quad (13)$$

which, for the maximum number of adsorbed molecules when  $dN_a/dt = 0$ , gives

$$N_{AD} = \frac{\alpha \gamma \phi_{10} t_{10}^n}{t^n} \tau \quad (\text{cm}^{-2}) \quad (14)$$

This equation indicates a sequence of equilibrium conditions. The molecules on the surface will be maximum when the flux is maximum at the earliest exposure, and the quantity is strongly affected by  $\tau = \tau_0 \exp E/RT_s$ . Although the molecules will be leaving the surface as the impinging flux decays, a number of them will remain. The number of molecules left depends on the binding energy that can be effective up to several monolayers, on the surface temperature, and on the residual flux. The time of maximum deposit,  $t_m$ , found previously is indicative of the time when the residual deposit will eventually be dictated by the adsorption process.

In all of the foregoing, the effects of radiation exposure on the deposited material, which may affect the energies of sublimation and desorption and the characteristics of the material, have been ignored because of lack of information.

Figure 14 is a plot of the time of maximum accumulation of a flux,  $\alpha \gamma \phi_{10}$ , which is decaying as  $t^{-3/2}$  and impinging on a surface at  $T_s$ . The flux is specified by: (1) the sticking coefficient, obtainable from literature; (2) the view factor,  $\gamma$ , calculable from geometry; and (3) the magnitude of the source,  $\phi_{10}$ , conveniently taken at  $t_{10} = 10$  hours in this case. The time is strongly dependent on the saturated vapor pressure  $P_s$  of the contaminant, corresponding to the surface temperature,  $T_s$ . The plot includes equivalent fluxes,  $\alpha \gamma \phi_{10}$ , varying from  $10^9$  to  $10^{17} \text{ cm}^{-2} \text{ s}^{-1}$  for contaminants considered to be  $\text{H}_2\text{O}$  and equivalent fluxes of DC-705 silicone oils varying from  $10^{12}$  to  $10^{17} \text{ cm}^{-2} \text{ s}^{-1}$ . The latter material is included as a representative of very low vapor-pressure materials. Their vapor pressures have been calculated from the Clapeyron equation,  $\ln P_s = A - B/T_s$ , with  $A = 10.48$  and  $B = 2680$  for  $\text{H}_2\text{O}$  and  $A = 12.11$  and  $B = 6424$  for DC-705. The times corresponding to 1-week and 1-month flights are shown for reference.

Figure 15 is a plot of the percent of accumulation on a surface as a function of time. It was obtained from equation 12c. It shows that 70 percent of the total is deposited within 10 hours and 90 percent is deposited in 100 hours. For a 1-week mission, the deposit is 92 percent, and for a 1-month mission, it is 96 percent of the full accumulation. Figure 16 shows the deposit ( $\text{cm}^{-2}$ ) or the thickness (cm) taken to be  $\text{H}_2\text{O}$  on a cryogenic surface as a function of time and equivalent flux. This was obtained from equation 12c with the second term assumed to be negligible.

Figure 17 shows the effect of delaying the exposure or cooling down of the surface. For a surface exposed 40 hours after the mission starts, the deposit will be about 9 percent of that expected in 1 week and 13 percent of that for 1 month. For comparison, the plot shows similar information for a source that decays linearly with time. A source decaying as  $t^{-1/2}$  will require longer delay times than the linear relation to provide the same reduction in deposits.

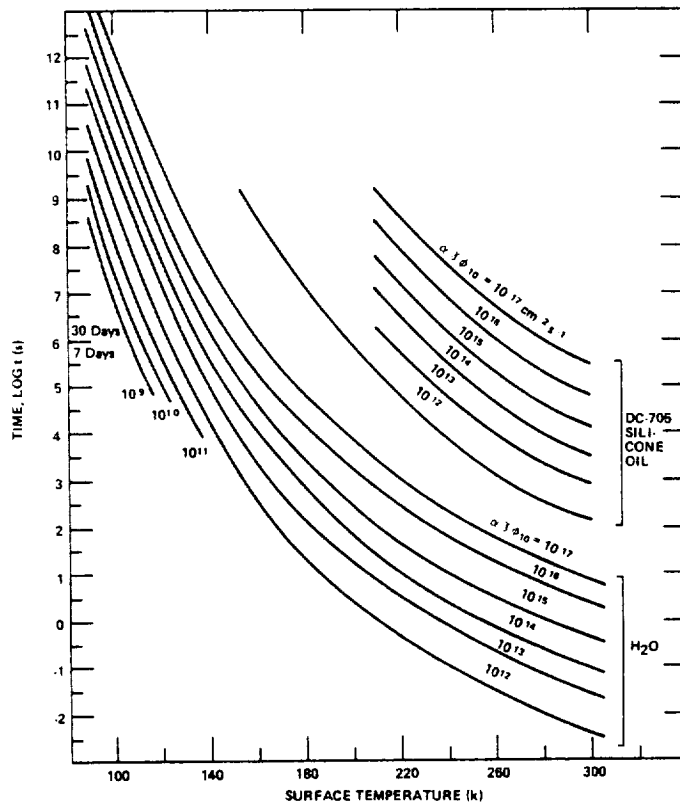


Figure 14. Time for maximum deposit of  $H_2O$  and DC-705 oil on a surface at  $T(K)$  for flux decaying as  $t^{-3/2}$  and having a value  $\alpha\gamma\phi_{10}$  at 10 hours.

## PREDICTED CONTAMINANT DEPOSITS ON SHUTTLE PAYLOADS SURFACES

Assuming that the Shuttle bay environment is dictated by payloads similar to the CTS-M or LMOP and that an instrument such as the CLIR telescope is among the payloads, the contaminant deposits on its critical surfaces can be estimated. The results of these calculations for a 200-km orbit are listed in table 2 and discussed in the following paragraphs.

### Early Stages of Flight

The gaseous conditions existing in the Shuttle bay during the early stage of flight with the door closed or open, can be estimated by using the equations or plots of Figures 10, 11, 12, and 13. Extrapolating the curves to 1 hour in flight, the following conditions should exist in the bay: density, about  $3.5 \times 10^{12} \text{ cm}^{-3}$ ; direct flux, about  $1.5 \times 10^{17} \text{ cm}^{-2} \text{ s}^{-1}$ ; column density,  $2.5 \times 10^{14} \text{ cm}^{-2}$ ; and return flux (with bay door open), about  $1.4 \times 10^{16} \text{ cm}^{-2} \text{ s}^{-1}$ . For convenience, Figure 18 is included to permit rapid conversion from molecular flux rates to mass flux rates. The indicated density at 1 hour corresponds to a pressure of about  $1.08 \times 10^{-4}$  torr. The contamination on a surface at 290 K that may occur during this period is estimated as follows. Figure 14 shows that, for  $H_2O$  fluxes of  $1.5 \times 10^{17}$ , the deposits on a 290-K surface occur for less than 100 seconds. Therefore, the

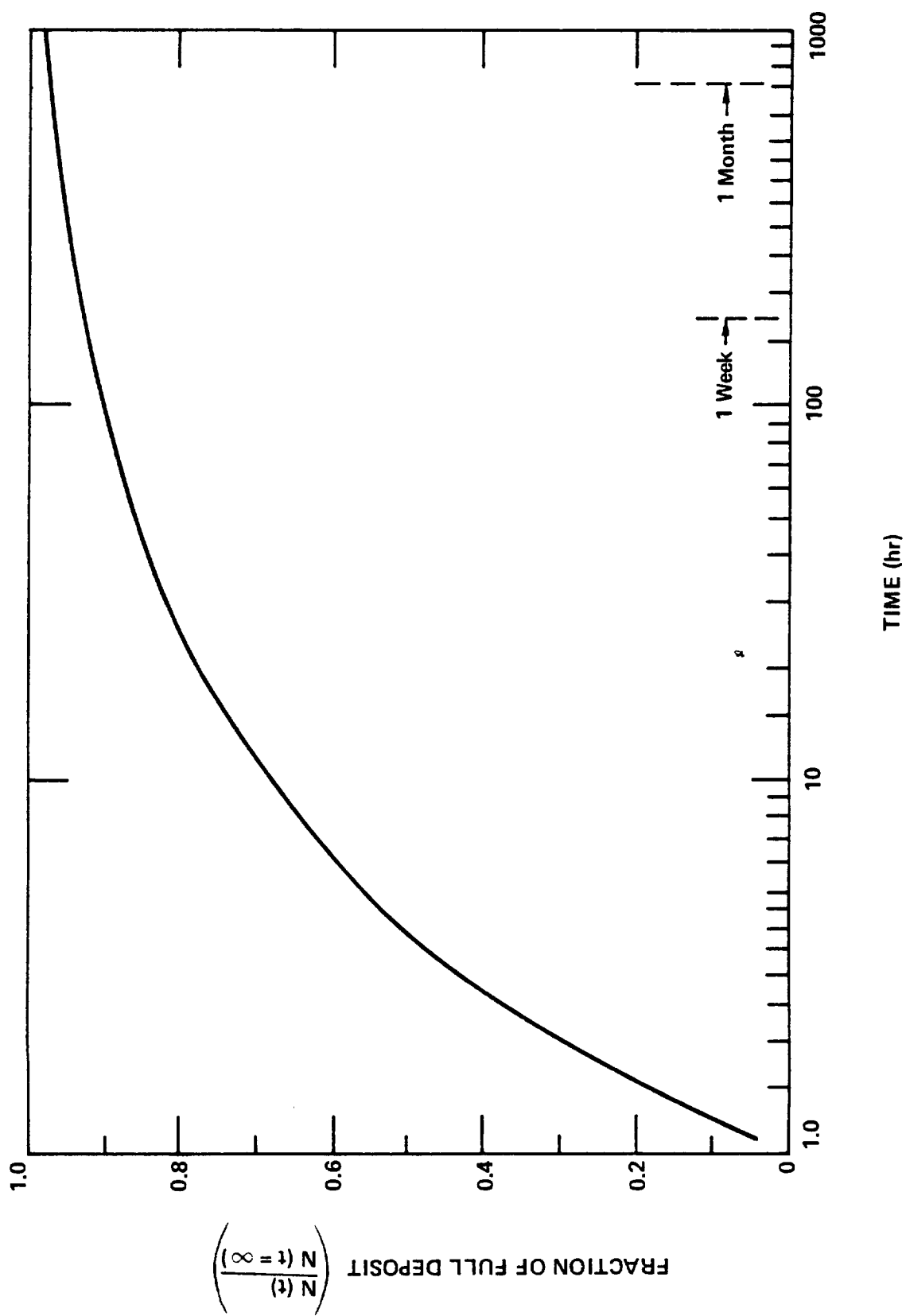


Figure 15. Fraction of full outgassing (deposit) versus time for source decaying as  $t^{-3/2}$ .

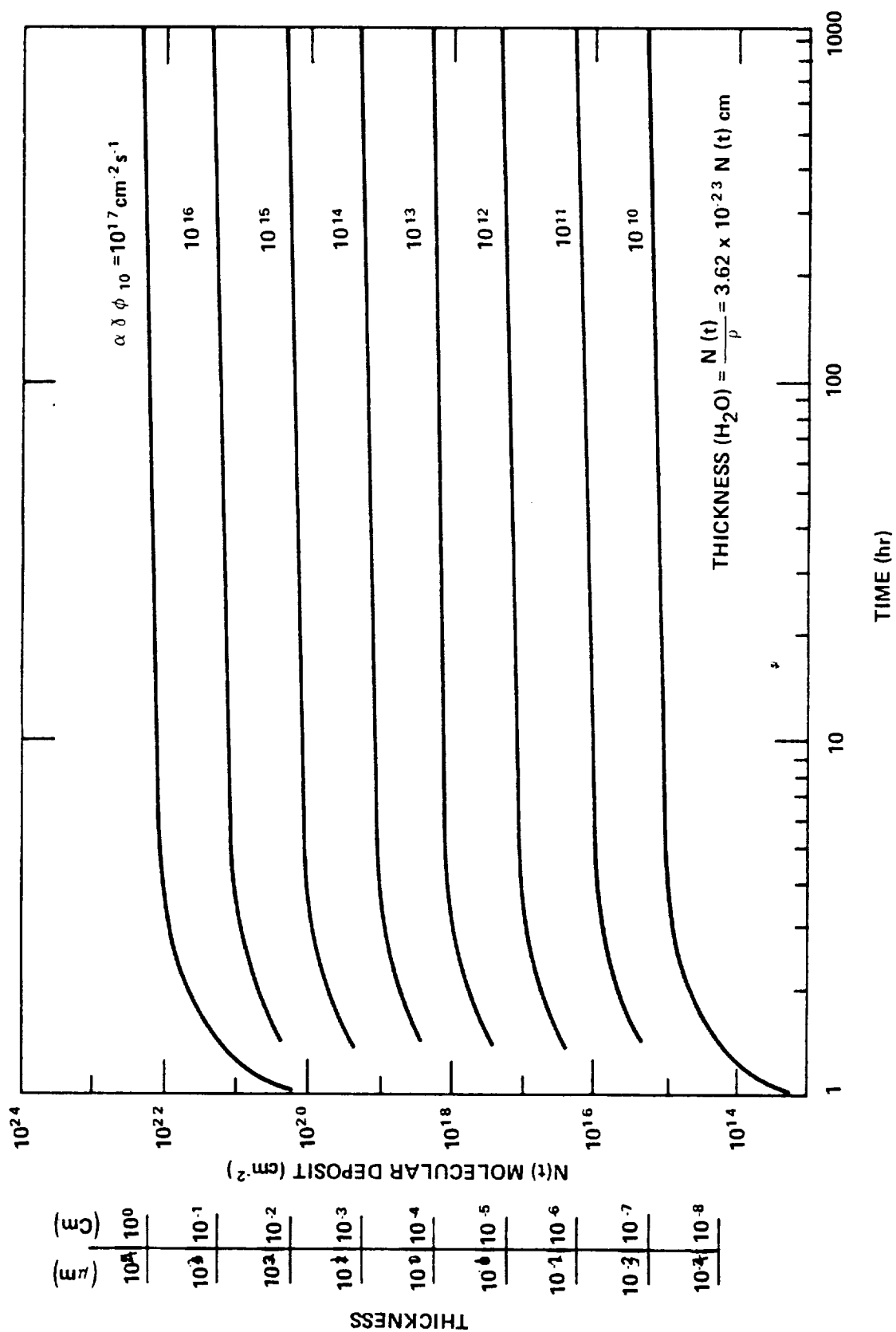


Figure 16. Maximum molecular deposit on surface versus time for contaminant flux decaying as  $t^{-3/2}$  and having a value  $\alpha\gamma\phi_{10}$  at 10 hours.



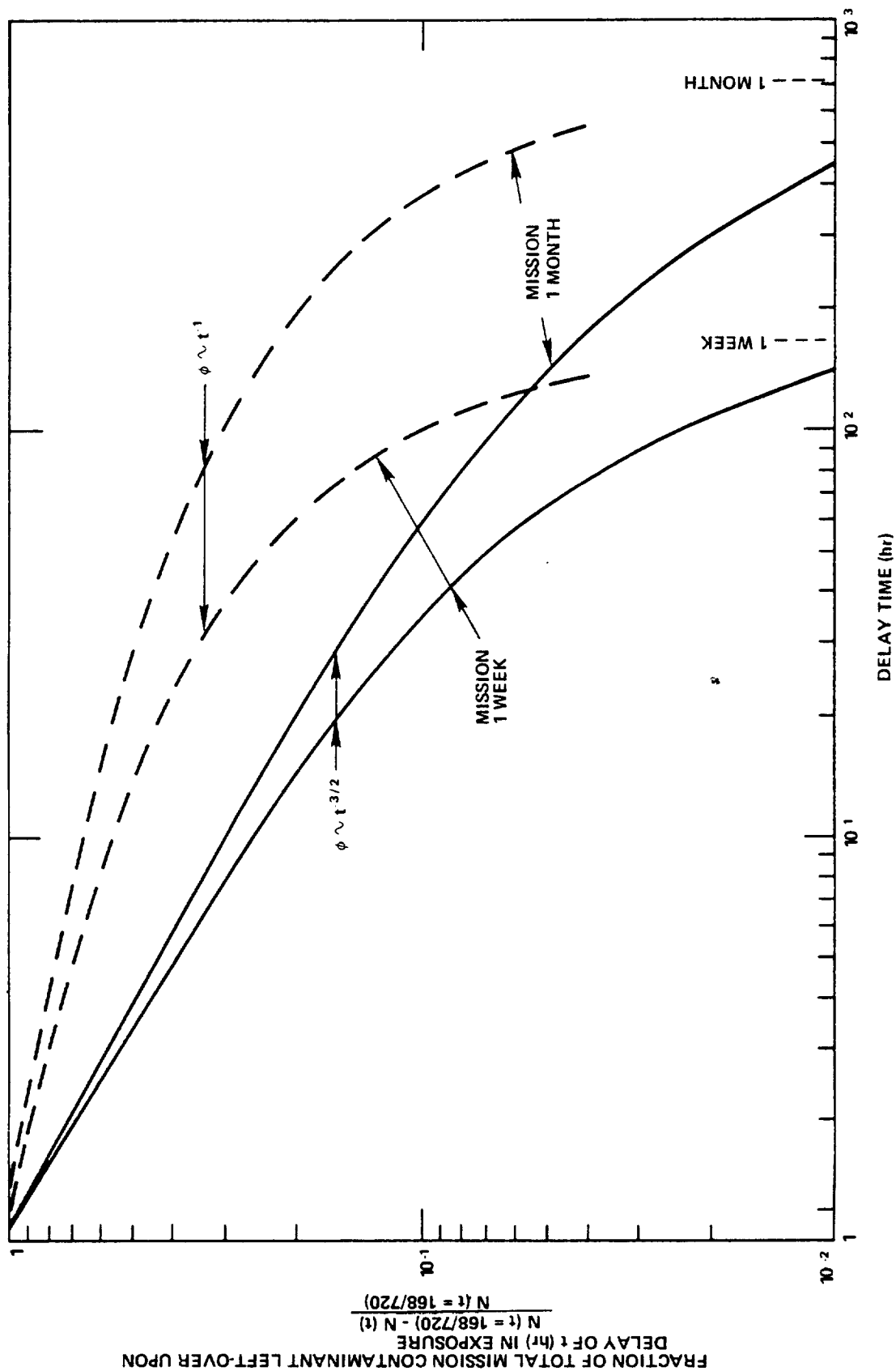


Figure 17. Fraction of total contaminant remaining when surface is exposed or cooled down  $t$  (hr) after mission starts.

**Table 2**  
**Instrument Contamination Predictions for Shuttle with LMOP/CTS-M-Type Payload at 200-km Orbit**  
**(Surface view factors:  $\gamma = 1$ , direct surface/CLIR telescope forward baffle;  $\gamma = 6.2 \times 10^{-2}$ , CLIR mirror)**

Gaseous Sources	Time in flight	Pressure (torr)	Density (cm <sup>-3</sup> )	Flux (cm <sup>-2</sup> s <sup>-1</sup> )	Column Density (cm <sup>-2</sup> )	Return Flux (cm <sup>-2</sup> s <sup>-1</sup> )	Deposit (cm) or Deposit Rate (cm/s)				Remarks
							$\gamma = 1.0$				
							$\gamma = 0.62$				
							Direct	Return	Direct	Return	
-Early outgas Closed bay door Open door 0.1% NVR <sup>(2)</sup>	1 hr	$(8 \times 10^{-4})^{(1)}$	$(2.6 \times 10^{13})$	$(3 \times 10^{17})$	$(2.5 \times 10^{14})$	$(1.4 \times 10^{16})$	$9.12 \times 10^{-5}$	$1.1 \times 10^{-6}$			on $T_s = 293$ K for $\sim 700$ s; $d = 10^{-3}$ d max after 191 hr
	1 hr	$(1 \times 10^{-4})$	$(3.5 \times 10^{12})$	$(1.5 \times 10^{17})$	$8 \times 10^9$	$5 \times 10^{11}$					
	1 hr	$(1 \times 10^{-7})$	$1 \times 10^8$	$5 \times 10^{12}$							
-Outgassing	1 hr-1 week		$1 \times 10^{11}$	$5 \times 10^{15}$	$8 \times 10^{12}$	$5 \times 10^{14}$	$5 \times 10^{12}$	$4.0 \times 10^{-3}$	$3.1 \times 10^{-3}$	$2.5 \times 10^{-4}$	on $T_s < 135.140$ K (on $T_s > 135$ K for $< 10^6$ s)
	1 hr-1 month		$1 \times 10^{11}$	$5 \times 10^{15}$	$8 \times 10^{12}$	$5 \times 10^{14}$	$5.5 \times 10^{12}$	$4.4 \times 10^{-3}$	$3.4 \times 10^{-3}$	$2.73 \times 10^{-4}$	
	40 hr-1 week		$1 \times 10^{11}$	$5 \times 10^{15}$	$8 \times 10^{12}$	$5 \times 10^{14}$	$4.5 \times 10^{13}$	$3.62 \times 10^{-4}$	$2.8 \times 10^{-4}$	$2.25 \times 10^{-5}$	
	40 hr-1 month		$1 \times 10^{11}$	$5 \times 10^{15}$	$8 \times 10^{12}$	$5 \times 10^{14}$	$6.8 \times 10^{13}$	$5.5 \times 10^{-4}$	$3.4 \times 10^{-4}$	$3.4 \times 10^{-5}$	
-VCS 0.1% NVR	Any		$(5 \times 10^{11})$		$(8 \times 10^{14})$	$(1.95 \times 10^{15})$		$5.8 \times 10^{-8}$ cm/s		$3.6 \times 10^{-9}$ cm/s	on $T_s < 150$ K indefinitely on $T_s = 293$ K indefinitely
	Any		$(5 \times 10^8)$		$(8 \times 10^{11})$	$(1.95 \times 10^{12})$		$1.6 \times 10^{-9}$ cm/s		$1.0 \times 10^{-10}$ cm/s	
-Evaporator	Any		$(1.5 \times 10^{11})$		$(4 \times 10^{14})$	$(8 \times 10^{14})$		$2.38 \times 10^{-8}$ cm/s		$1.48 \times 10^{-9}$ cm/s	on $T_s < 140$ K indefinitely
-Ambient oxygen in velocity vector	Any	$(P_e = 1.4 \times 10^{-5})$	$(4 \times 10^9)$	$(3.2 \times 10^{15})$			$\alpha = 1$	$7.5 \times 10^{-8}$			on $T_s < 35$ K
							$\alpha = 1.37 \times 10^{-2}$	$1.0 \times 10^{-9}$ cm/s			

<sup>(1)</sup>Numbers in parenthesis indicate values at that time; others are values at 10 hours.

<sup>(2)</sup>NVR = Non volatile residues (DC-705 silicone oil).

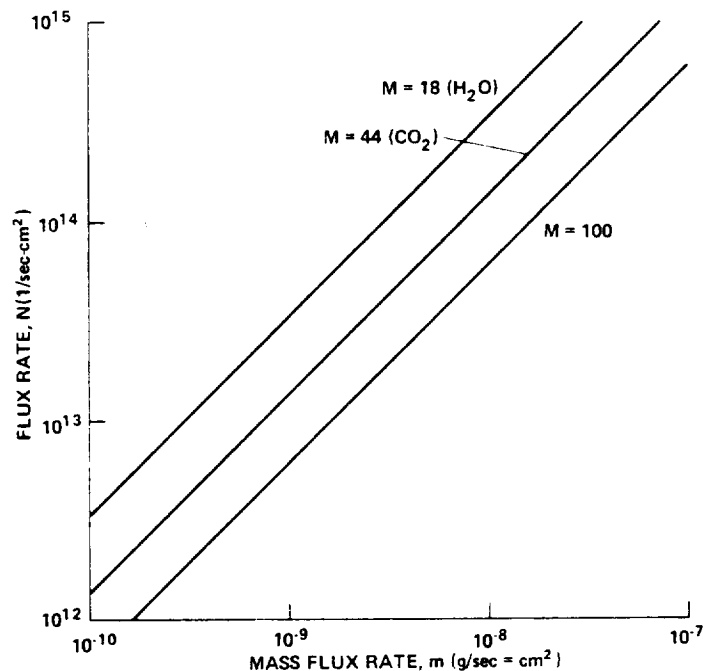


Figure 18. Conversion data from the mass flux rate,  $m$ , to the number flux rate,  $N$  ( $1/\text{cm}^2\text{-sec}$ ).

maximum deposit is about  $10^{19} \text{ cm}^{-2}$  or less than  $10^5$  monolayers of  $\text{H}_2\text{O}$ . After 100 seconds, these monolayers evaporate quite rapidly because of the high  $\text{H}_2\text{O}$  vapor pressure at 290 K, but the surface may retain a few monolayers by virtue of surface forces.

However, if the foregoing flux includes a fraction, say 0.1 percent, of the so-called volatile condensable materials (VCM) as per material selection criteria, this material will accumulate on a 290-K surface. The accumulation should last for a period of  $7.7 \times 10^2$  seconds, as shown by Figure 14 for a DC-705 flux,  $\alpha\gamma\phi_{10}$ , at 10 hours of  $5 \times 10^{12}$  (Figure 12). The deposit will be about  $9.12 \times 10^{-5} \text{ cm}$  thick because the direct flux of this material has a value of  $1.5 \times 10^{14}$  at 1 hour. In addition, when the bay door is open, the return flux, which, for VCM material, has a value at 10 hours of  $5 \times 10^{11}$  (Figure 13), contributes to the deposit. The deposit of this flux should continue for  $10^2 \text{ s}$ , and the deposit will be  $1.1 \times 10^{-6} \text{ cm}$  on the exposed surfaces at 290 K. Thereafter the total VCM deposit thickness of  $9.2 \times 10^{-5} \text{ cm}$  will decrease with time. After a week to 191 hours, the thickness should be about  $9.2 \times 10^{-8} \text{ cm}$ . This was calculated using equation 8 for  $E = 25 \text{ kcal/mole}$  and  $T_s = 290 \text{ K}$ , resulting in a residence time of  $10^5 \text{ s}$ .

### Outgassing Deposits on Cryogenic Surfaces

The outgassing direct flux at 10 hours is about  $5 \times 10^{15} \text{ cm}^{-2} \text{ s}^{-1}$  (Figure 12), and the return flux at 200 km at the same time is about  $5 \times 10^{14}$  (Figure 13). Neither of these sources will accrete on normal-temperature surfaces as shown by Figure 14, which indicates a very short  $t_m$ . But, for a sur-

face at less than 140 K, the time of accumulation is longer than a 1-week or 1-month mission. The total accumulation can be obtained from Figure 16. In fact, the deposit for the direct flux ( $\alpha\gamma\phi_{10} = 5 \times 10^{15}$ ) for a 1-week mission will be  $5 \times 10^{-2}$  cm. The return flux ( $\alpha\gamma\phi_{10} = 5 \times 10^{14}$ ) will produce a thickness of  $4 \times 10^{-3}$  cm during the same period. This thickness could result at the forward baffle of the telescope where the temperature is less than 140 K.

The corresponding deposits on surfaces with a view factor of  $\gamma=6.2 \times 10^{-2}$ , such as those for the CLIR telescope, will be  $3.1 \times 10^{-3}$  cm for the direct flux ( $\alpha\gamma\phi_{10}=3.1 \times 10^{14}$ ) and  $2.5 \times 10^{-4}$  cm for the return flux ( $\alpha\gamma\phi_{10}=3 \times 10^{13}$ ). These deposits will be about 10 percent higher for a 1-month mission, as shown in Figure 15. To show the effect of delaying the exposure on the cooling down of the surfaces, table 2 shows the deposits calculated for a delay of 40 hours. They are approximately one order of magnitude lower than those calculated for the immediate exposure at 1 hour. Figure 17 shows the delaying effect. Note that the foregoing calculations were made assuming  $H_2O$  as the gaseous fluxes. However, according to Figure 14, they are valid for any material with vapor pressures less than those of  $H_2O$ . If the surfaces are at  $T_s > 140$  K, the accumulations could terminate before the end of the mission. The calculations would be carried out in the same manner using Figure 14 to obtain  $t_m$ , and Figure 16 or equation 12c to obtain maximum deposits for a span of time  $t_m$ .

### Deposit Rates of VCS and Evaporator Products

Return fluxes from the evaporator and VCS at 200-km orbits are  $8 \times 10^{14}$  and  $1.95 \times 10^{15} \text{ cm}^{-2} \text{ s}^{-1}$ , respectively, as shown in Figure 13. The  $H_2O$  from the evaporator will deposit at a rate of  $2.38 \times 10^{-8}$  cm/s on a cryogenic surface  $T_s < 140$  K with direct view of the flux, such as that of the forward baffle of the telescope. The deposit rate on the mirror ( $\gamma=6.2 \times 10^{-2}$ ) will be  $1.48 \times 10^{-9}$  cm/s. The corresponding rates for the VCS products are  $5.8 \times 10^{-8}$  and  $3.6 \times 10^{-9}$  cm/s, respectively. These magnitudes are of the order of monolayers per second. There will be no deposits on surfaces at  $T > 140$  K of the mostly  $H_2O$  content of the outgassing products. However, if the VCS products are estimated to contain a 0.1-percent low-vapor-pressure material, they could deposit at a rate of  $1 \times 10^{-10}$  cm/s on a surface with  $\gamma=6.2 \times 10^{-2}$  field of view and  $1.6 \times 10^{-9}$  cm/s on a direct-view surface.

### Oxygen Deposits on Cryosurfaces

At 200 km, the natural concentration of O is  $4.05 \times 10^{15} \text{ m}^{-3}$  and  $O_2$  is  $1.91 \times 10^{14} \text{ m}^{-3}$  (Reference 13). The average velocities of O and  $O_2$  are 1.5 km/s and 1.08 km/s, and their temperatures vary between 900 K at night and 1600 K during the day. For a pseudomaxwellian flux distribution, the flux at the mirror of the telescope pointing in the direction perpendicular to the velocity vector will be  $\phi=1/4\rho V\gamma$ . For  $\rho=4 \times 10^{15}$ ,  $V=1.5$  km/s and  $\gamma=6.2 \times 10^{-2}$ , the flux is  $9.3 \times 10^{12} \text{ cm}^{-2} \text{ s}^{-1}$ , which corresponds to a pressure of  $4.58 \times 10^{-8}$  torr as per Langmuir equations with  $T=1500$  K and  $M=16$ . Because the vapor pressure of  $O_2$  at 30 K is about  $1.2 \times 10^{-7}$  torr, accumulation of oxygen should not occur at the mirror-surface temperature or on surfaces at 100 K. If, however, the telescope is pointed along the velocity vector, the oxygen flux on any surface of the telescope is  $\rho V = 3.2 \times 10^{15} \text{ cm}^{-2} \text{ s}^{-1}$  where  $V=8$  km/s. This is equivalent to  $1.4 \times 10^{-5}$  torr. Consequently, it should

accrete on surfaces at  $T_s < 35$  K at a rate dictated by the sticking coefficient. For the unity coefficient, the rate is about  $7.54 \times 10^{-8}$  cm/s. Reference 16 indicates that the sticking coefficient  $c_o$  of  $O_2$  at temperature  $T_g = 300$  K on a surface at  $T_s = 20$  K is 0.86. Further, Reference 16 gives the relation  $(1-C)^T = (1-C_o)^{T_g}$  for the evaluation of  $C$  at a temperature,  $T$ , of the gas for the same surface temperature. Assuming that the temperature of the gas is proportional to the square of its velocity, the temperature of the oxygen at 8 km/s could be equal to 42666 K. The sticking coefficient from the foregoing relation can be calculated to be  $1.37 \times 10^{-2}$ , and the O accretion rate in this case could be  $1.02 \times 10^{-9}$  cm/s. The heat inputs produced by these fluxes to the surface was estimated to be about  $2.2 \times 10^{-7}$  cal/cm<sup>2</sup>/s, which are equal to the emissive power of a blackbody at 20 K (Reference 15).

## METHODS FOR REDUCING CONTAMINATION

The following paragraphs describe some of the measures that can be used for alleviating the contamination predicted previously. The discussion of these measures is complemented with a list of suggested design and operational contamination controls. The methods of contamination control discussed in detail are: (1) purging the telescope; (2) periodic sublimation of deposited materials; and (3) time required for protecting the surfaces both during and after operation of the evaporator and the VCS systems.

### Gaseous Purging

To protect the telescope mirror and baffle from incoming natural oxygen or other materials, one may employ He gas vented by the telescope at 100 K as a counterflow to the contaminant. The amount of He needed for the purging to be effective must now be estimated. The traverse time of the incoming O to reach the mirror is  $L/V$ , where  $L$  is the telescope tube length and  $V$  is the spacecraft velocity. To prevent the molecules from reaching the mirror, the mean collision of the gases in the tube should be several times less than the traverse time. The mean free path (mfp) of the purging gas should be

$$\lambda_p < \frac{L}{V} \quad v \quad (15)$$

where  $v = \sqrt{8RT/\pi m} = (1.45 \times 10^4) \times \sqrt{T/M}$  (cm/s) is the average velocity of the purging He, which, at 100 K corresponds to a velocity of  $7.25 \times 10^4$  cm/s. Therefore, for  $L=100$  cm,  $V=8$  km/s, and the He velocity as above, the mfp should be less than 9 cm. From the kinetic theory, the mfp of a gas is given by

$$\lambda = \frac{KT}{\sqrt{2} \pi \sigma^2 P} \quad (\text{cm}) \quad (16)$$

where  $K$  is the Boltzman constant,  $\sigma$  is the cross section of the molecule, and  $T$  and  $P$  are its temperature and pressure, respectively. With the appropriate constant and cross section of the He, the equation reduces to  $\lambda = 4.89 \times 10^{-5} T/P$  (cm), where  $T$ (k) and  $P$ (torr). Equating the two mfp relationships, the required pressure for the purging gas is

$$P > \frac{1}{\sqrt{2} \pi \sigma^2} \frac{V}{L} \sqrt{\frac{\pi M K T}{8 N}} > 3.37 \times 10^{-9} \frac{V}{L} \sqrt{MT} \quad (\text{torr}) \quad (17)$$

With the specified geometry and gas, the above indicates that the pressure should be greater than  $5.4 \times 10^{-4}$  torr. The throughput of a gas at pressure  $P$  through a tube of area  $A$ , diameter  $D$ , length  $L$ , and velocity  $V$  can be estimated as:

$$Q = \frac{4}{3} \frac{D}{L} \left( \frac{1}{4} A v \right) \frac{P}{KT} \quad \left( \frac{\text{torr } \ell}{s} \right) \quad (18)$$

This equation for  $D=25$  cm,  $A=487$  cm<sup>2</sup>,  $L=100$  cm,  $T=100$  K,  $v=7.25 \times 10^4$  cm/s and  $P=5 \times 10^{-4}$  torr, indicates a requirement of more than 1.6 torr  $\ell/s$ . This corresponds to a mass flow rate,

$$\dot{m} = \frac{QM}{P_0 V_0} = 3.75 \times 10^{-4} \text{ g/s} \quad (19)$$

where  $P_0=760$  torr,  $V_0=22.4$   $\ell/\text{mole}$ , and  $M=4$  g/mole. Therefore, for some beneficial effects of the purging with He at 100 K, a flow greater than 32.5 g/day is required.

### Sublimation of Condensed Oxygen

During operation of the telescope, natural oxygen condenses on optical surfaces at  $T < 30$  K. The temperature and time required for subliming a given accumulation from the surface must now be estimated.

The rate of removal of molecules,  $\phi_L$ , from a surface at  $T_L$  is the difference between the rate of sublimation,  $\phi_L$ , and the rate of molecules impinging on the surface; i.e.,

$$\sigma_L = \phi_L - \phi_i = \phi_L \left( 1 - \frac{\phi_i}{\phi_L} \right) = \frac{P_L}{17.14} \sqrt{\frac{M}{T_L}} \left( 1 - \frac{P_i}{P_L} \sqrt{\frac{T_L}{T_i}} \right) \quad (\text{gcm}^{-2} \text{ s}^{-1}) \quad (20)$$

Equation 20 is obtained by using the Langmuir equation. The oxygen flux on the mirror at an altitude of 200 km was previously calculated to be equal to  $P_i = 1.4 \times 10^{-5}$  torr. The pressure,  $P_L$  (torr), and temperature,  $T_L$  (K), are the saturated vapor pressure and temperature of the oxygen. At  $T_L$

=40 K,  $P_L$  is about  $10^{-3}$  torr, which is much greater than the equivalent impinging pressure of  $P_L = 1.4 \times 10^{-5}$  torr. At a 40-K surface, the oxygen will not condense but will leave at a rate

$$\sigma_L = \frac{P_L}{17.14} \sqrt{\frac{M}{T_L}} = 3.68 \times 10^{-5} \text{ (gcm}^{-2} \text{ s}^{-1}) \quad (21)$$

As previously indicated, oxygen condensation for 1 day was estimated to be  $6.48 \times 10^{-3}$  cm/day  $= 5.76 \times 10^{-3}$  g/cm<sup>2</sup> day for the unit sticking coefficient. Therefore, the time required for subliming a 1-day accumulation with a surface at 40 K will be about 156 seconds.

### Waiting Time After VCS and Evaporator Operation

An estimate of the time one should wait after the operations of these systems so that their scattering fluxes and column densities become acceptable, can be obtained as follows. The column density,  $N$ , can be expressed as

$$N \approx \frac{\dot{N}}{4\pi v R} \quad (\text{cm}^{-2}) \quad (22)$$

where  $\dot{N}$  (s<sup>-1</sup>) and  $v$  (cm s<sup>-1</sup>) are the effluent rate and its velocity, and  $R$ (cm) is the reference radius of the source. If the reference radius is assumed to be increasing linearly as  $R=R_0+vt$ , the column density,  $N$ , at time,  $t$ , is related to the column density,  $N_0$ , corresponding to radius  $R_0$  as:

$$N = \frac{N_0}{1 + vt/R_0} \quad (23)$$

Hence, an instrument that is  $R_0=6$  m away from a source with an effluent velocity of  $v=530$  m/s will see a column density of  $10^{-4}N_0$  about 1 minute after the source effluent was terminated. Waiting this time before exposing an instrument or making measurements should provide both good observations and protection from contamination.

### DESIGN AND OPERATIONAL CONTAMINATION CONTROL

From the previous analysis, it is apparent that contamination hazard is greatest during the early hours of flight and while the evaporator and VCS are being used. Considerable amounts of contaminants, including ambient oxygen, will collect on cryogenic surfaces. The magnitude of the deposits can be substantially reduced if certain design and operational precautions are taken. Some of these are:

- Protect cryogenic surfaces with dust covers and doors to inhibit ingestion of gases and particles and to limit the exposure to periods when the environment is acceptable.

- Monitor the gaseous environment with instruments that simulate the temperature of the critical surface. Instruments suitable for this purpose may be quartz crystal microbalances, water vapor radiometers, and calorimetric devices. They can measure the molecular flux rate to determine the advisability of exposing the critical surface.
- Include internal monitoring (e.g., inside a telescope) to provide data on total deposit. These data can be used for recalibrating an instrument.
- Provide energy sources that can be used to maintain a surface at elevated temperatures and to sublime existing contaminant deposits.
- Use cryogases to purge the system. This may prevent some contaminant molecules from reaching the surface.
- Sufficiently vent insulation materials, lubricated motors, and other sources away from critical surfaces.
- Expose systems and materials to vacuum, bake, and purging before using them in space, preferably a short time before.
- Select materials with low outgassing, as determined from actual tests on their rates of outgassing versus time, or, if this is not possible, utilize VCM material selection tests. Note that the VCM test does not provide outgassing rates or ensure<sup>3</sup> that the material will be acceptable in actual use.
- Extend the entrance of a telescope or probe as far as possible from the bay where the density is lower. This is more effective at low-orbit altitudes.
- Gimbal-mount pointing instruments so that they remain fixed to the object while the Shuttle is changing attitude. This can prevent the instrument from pointing in the velocity vector and reduce the VCS operations.
- Use gravity-gradient altitude flights so that there will be fewer VCS/RCS firing.
- Use flights with lower bay temperatures because outgassing is strongly dependent on temperature.
- Use flights with lower power requirements to reduce the amount of water generated by the power cells, and, hence, the number of flash evaporator operations, or use flights that carry ample water-storage capabilities.
- When acceptable, use high-altitude flights because the ambient scattering return fluxes are an order of magnitude lower at 400 km than at 200 km, there is less chance of contamination.



- Do not point instruments in the velocity vector because the return fluxes are maximum in the velocity vector. Also, avoid looking toward the Shuttle cabin. Some water vapor will be escaping through the structural joints of the cabin.
- Avoid measurements and critical surface exposure during RCS/VCS and evaporator operations or other intentional venting. Wait 2 or 3 minutes after these operations before uncovering instruments and making measurements.
- Delay cool-down, exposure, and measurements for as many hours as possible. For example, exposing a surface 40 hours after flight initiation can reduce contaminant deposits by about 90 percent.
- Use dedicated flights that include instruments and payloads concerned with contamination.
- Use previously flown Shuttles, preferably those that have been recently flown. They have been exposed to vacuum and degassed, especially of highly volatile materials. Avoid recently retiled orbiters.
- Monitor fluxes at the instrument entrance because the flux rates at that location are a measure of the column density and of the degree of contaminant hazard. Variable temperature monitors can be used to obtain information on the nature of the contaminant.
- Use the results of the induced-environment contamination monitor (IECM). This package of instruments, designed for mapping and measurement survey during several early flights, may indicate a best location for the instrument.
- Investigate synergistic effect of other payloads on the instrument. Perform detailed analysis on the environment at the instrument location. A knowledge of the sources outgassing, their temperatures, their view factors, contaminant transport mechanisms, operational modes, etc. is necessary.
- Be informed in advance of flight plans or obtain real-time information on RCS/VCS/evaporator and other venting operations so that protective actions can be taken.

## SUMMARY OF THE RESULTS

With reference to the various plots and Table 2, the environment and contamination prediction for payloads in the Shuttle bay can be summarized as follows:

While the bay doors are closed, the pressure is of the order of  $10^{-3}$  -  $10^{-4}$  torr within 1 hour of the beginning of the flight. With the doors open, the pressure should be about  $10^{-4}$  torr in the vicinity of the payloads, and the column density should be about  $2.5 \times 10^{14} \text{ cm}^{-2}$ . During the 1 to 2 hour transition period, surfaces at room temperatures should acquire a few monolayers of  $\text{H}_2\text{O}$  retained

by surface forces. For a short period of 10 to 15 minutes, however, about  $10^{-5}$  -  $10^{-6}$  cm of low vapor-pressure materials (VCM) should accumulate on these surfaces. This material will leave very slowly and, at the end of 1 week of flight, should be about  $10^{-8}$  cm or less. If the surfaces are cooler than 290 K, this material will continue to accumulate for a longer period and its release will be correspondingly much slower.

Directly exposed surfaces at  $T < 135$  to 140 K will be covered with a  $5 \times 10^{-2}$  cm thick deposit after a 1-week flight or 10 percent more after a 1-month flight. For a cold surface as above, but having a  $6.2 \times 10^{-2}$  view factor as for the CLIR mirror, the foregoing deposits are reduced in proportion. With the telescope deployed beyond the bay area, the scattered flux deposits a thickness of  $4 \times 10^{-3}$  cm on the forward baffle and  $2.5 \times 10^{-4}$  cm on the mirror for the 1-week flight. If the cool-down or exposure is delayed by 40 hours, the foregoing deposits will be about 9 percent of the above. Column densities on the order of  $10^{12}$  cm $^{-2}$  should be established 30 to 40 hours into the flight.

While the evaporator and the VCS are operating, the column densities are  $10^{14}$  -  $10^{15}$  cm $^{-2}$ . The return flux of the VCS at 200 km will deposit at a rate of about  $5.8 \times 10^{-8}$  cm/s on a surface at  $T < 150$  K with direct field of view and at about  $3.6 \times 10^{-9}$  cm/s on the telescope mirror. The water constituent of the VCS will not accrete on a surface at room temperature. However, its estimated 0.1% content of VCM will accrete at a rate of  $1.6 \times 10^{-9}$  cm/s on these surfaces ( $1 \times 10^{-10}$  cm/s on surfaces with a  $6.2 \times 10^{-2}$  field of view).

The 100-percent water constituent of the evaporator will condense at  $T_s < 140$  K at a rate of  $2.38 \times 10^{-8}$  on direct surfaces and at a rate of  $1.48 \times 10^{-9}$  cm/s on surfaces with  $\gamma = 6.2 \times 10^{-2}$ .

With regard to the ambient oxygen, if the telescope is pointed in the velocity vector, it will deposit on surfaces at  $T < 35$  K at a rate between  $7.5 \times 10^{-8}$  and  $1 \times 10^{-9}$  cm/s, depending on the sticking coefficient.

Although directional fluid leaks, improper direct venting of compartments, coolant leaks, motor leaks, etc. have not been considered, they would increase the contaminant hazard.

In addition to postponing as long as possible the exposure or the cool-down of the critical surface, the contamination can be minimized by: (1) exposing the surface to a noncontaminating gaseous purging flow; (2) periodically subliming the contaminant deposits; (3) protecting the surface during gaseous emissions (VCS/evaporator) and (4) reexposing the surface after the environment returns to normal. To minimize the ingestion of natural oxygen and other contaminants in the telescope, vented He gas at 100 K can be used as a counter flow to the contaminants. For the CLIR telescope and for an orbit of 200 km, the He pressure in the telescope tube should be greater than  $5 \times 10^{-4}$  torr. This can be accomplished by providing an He flow greater than 32 g/day.

The calculated daily accretion of oxygen on the telescope mirror at 30 K ( $5.7 \times 10^{-3}$  g/cm $^2$ /day) can be removed by heating the surface to 40 K for about 3 minutes. This assumes that the surface and the deposited oxygen have not been changed by a chemical surface reaction aided by impinging radiations. The waiting period for resuming observations and surface exposure after the operation of the VCS/evaporator and other emissions is estimated to be about 2 minutes.

## CONCLUSIONS

The gaseous environment in which payloads and instruments will be exposed in the bay of the Shuttle Orbiter has been predicted. The prediction is based on the Shuttle discrete-time calculated molecular environment, and the measured, time-varying environment produced by a number of spacecraft in large vacuum chambers. The environment includes molecular density, directional fluxes, column density, and scattering fluxes contributed by material outgassing and emissions from the vernier control system and flash evaporator. These parameters are developed for different orbit altitudes and as a function of time. These predictions indicate that, with the exception of periods when the attitude motors and the evaporator are being used, the environment of a payload is dictated by the onboard payloads. It is also concluded that this environment is not significantly affected by the number of payloads in the bay. Rather, it is controlled by its self-induced environment or the maximum source nearby. The predictions provide representative environments that can be expected at a payload and estimate the times when certain recommended environmental criteria are met. The data can be used to estimate the degree of contamination that may result on critical surfaces. In fact, on the basis of a maximum estimated environment, contamination deposits have been calculated for a flight lasting 1 week or 1 month and for cryogenic and normal surface temperatures. These predictions include the effects of the field of view, the sticking coefficient, and the nature of the contaminant. For this purpose, a generalized method of estimating the deposits has been developed. It requires a knowledge of the source magnitude at a known time, its decay function, its chemical nature, and the temperature of the surface being contaminated. A specific calculation for the environment and the expected contaminant deposits on the surfaces of the CLIR have been performed and discussed. Included are an estimate of the rates of natural oxygen on the telescope optical surfaces and the effect of delaying the exposure or cool-down on the total deposits. Methods of reducing contamination, such as He purging of the telescope, sublimation of accumulated deposits, and time required for normalization of the environment after large gaseous emissions, have been investigated. These and other methods that can be used in designing and during flight operations have been listed.

In conclusion, in the absence of more detailed calculations to be performed later when more is known on the Shuttle and the specific payloads, this document has attempted to: (1) provide a general characterization of the molecular environment of the payloads in the bay of the Shuttle, (2) provide methods for estimating the degree of contamination on critical surfaces, and (3) indicate methods for alleviating it.



## REFERENCES

1. Anon., "Space Shuttle Program, Space Shuttle System Payload Accommodations," JSC-07700, Volumes X and XIV, Rev. C, Lyndon B. Johnson Space Center, July 3, 1974.
2. Leger, L., S. Jacobs, and H. K. F. Ehlers, "Space Shuttle Contamination Overview," *Journal of Environmental Sciences*, September-October 1978.
3. Rantanen, R. O., and D. A. Strange-Jensen, *Orbiter/Payload Contamination Control Assessment Support*, NASA CR151365, 1977.
4. Scialdone, J. J., *Self-Contamination and Environment of an Orbiting Spacecraft*, NASA TND-6645, May 1972.
5. Bareiss, L. E., "Verification Approach for the Shuttle/Payload Contamination Evaluation Program—Space-Lab Induced Environment," *Paper 78-1606, AIAA/IES/ASTM 10th Space Simulation Conference, Bethesda, Maryland*, October 16-18, 1978.
6. Rantanen, R. O., and D. A. Strange, "Shuttle Orbiter—IUS/DSP Satellite Interface Contamination Study," Final Report, Contract NAS9-15335, March 1978.
7. Scialdone, J. J., *Time Dependent Polar Distribution of Outgassing from a Spacecraft*, NASA TND-7597, April 1974.
8. Scialdone, J. J., *Gas Flow Analysis During Thermal Vacuum Test of a Spacecraft*, NASA TND-7492, January 1974.
9. Scialdone, J. J., "The Outgassing and Pressures in a Spacecraft," *Proceedings Institute of Environmental Sciences—20th Annual Meeting, Washington, D.C.*, April-May 1974, p. 164.
10. Henry, R. P., "Mesure Des Taux De Degazage," *Le Vide*, No. 144, November-December 1969, p. 316.
11. Liu, C. K., and A. P. Glassford, Kinetics Data For Diffusion of Outgassing Species from RTV 560 Silicone Rubber. *Journal of Vacuum Science and Technology*, 15 (5) September/October, 1978, p. 1761.
12. Scialdone, J. J., *Correlation of Self-Contamination Experiments in Orbit and Scattering Return Flux Calculations*, NASA TND-8438, March 1977.

13. Anon., "U.S. Standard Atmosphere, 1976," National Oceanic and Atmospheric Administration/NASA/USAF, October 1976.
14. Anon., "Cryogenic Limb-Scanning Interferometer and Radiometer (CLIR)," Report of the Spectroscopy Facility Definition Team, NASA/Goddard Space Flight Center, Greenbelt, Maryland, April 1978.
15. Murakami, M., *Theoretical Contamination of Cryogenic Satellite Telescope*, NASA TP-1177, April 1978.
16. Dawson, J. P., "Prediction of Cryopumping Speeds in Space Simulation Chambers," *Journal Spacecraft*, 3 (2) February 1966, p. 218.